A Comprehensive Understanding of Bainite Phase Transformation Mechanism in TRIP Bainitic-supported Ferrite Steel

Van Nhanh Nguyen [a], Anh Xuan Nguyen [b], Dinh Tuyen Nguyen [c], Huu Cuong Le [d], Van Phuc Nguyen [d,*]

[a] Institute of Engineering, HUTECH University, Ho Chi Minh city, Vietnam
[b] School of Mechanical Engineering, Vietnam Maritime University, Haiphong, Vietnam
[c] PATET Research Group, Ho Chi Minh city University of Transport, Ho Chi Minh city, Vietnam
[d] Institute of Maritime, Ho Chi Minh city University of Transport, Ho Chi Minh city, Vietnam
Corresponding author: *phuc.nguyen@ut.edu.vn

Abstract— **Mechanical parts on ships and automobiles are diverse in shape, size, and working conditions. They operate with static, cyclic, and shock loads in various environments at low and high temperatures. Therefore, materials need to be highly durable to ensure the reliability of parts and structures on ships and automobiles. Currently, materials used in the shipbuilding and automotive industry are diverse, and steel is commonly used. Therefore, the shipbuilding and automotive industry requires increasingly higher steel mechanical properties. Among the advanced high-strength steel families, low Mn steels with phase change, thanks to the plastic deformation process, are steel lines with high durability, flexibility, and good fatigue resistance. Therefore, low Mn steel is suitable for manufacturing load-bearing parts that undergo deformation to create the required shape. This work presents general studies on the effects of some elements, such as Mn, Si, and C, on the microstructure and mechanical properties of TRIP steel. This article also presents the mechanism of the phase transformation process of TRIP steel when heated and cooled under some conditions, the thermodynamic basis of the formation of TRIP-type bainitic ferrite steel structure, and the influence of C, Mn, and Si on the formation kinetics of TBF steel structure. Through these review studies, the article synthesizes and identifies a number of phase transformation mechanisms for steel; the influence of certain alloying elements on the microstructure and mechanical properties of steel has been determined.**

Keywords— **Bainite phase; transformation mechanism; TBF steel; mechanical properties; low-Mn steel.**
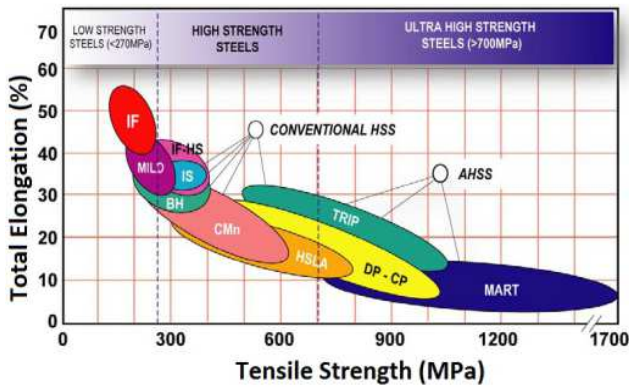
I. INTRODUCTION

The shipbuilding and automotive industry recently had great opportunities to gradually recover and grow production when shipping and automotive activities are recovering strongly [1]. Thus, developing supporting industries is one of the solutions to promote the development of the shipbuilding and automotive industry, in which the development of supporting industries in the shipbuilding and automotive industry requires the coordination and linkage of the mechanical industry, metallurgy, and chemicals [2], [3]. For the shipbuilding and automotive industries, material technology, including welding technology and welding treatment [4]–[7], nonferrous alloy [8]–[12], thermochemical treatment to increase durability [13]–[17], composite [18], [19], and finding new materials with high-durability and good-mechanical properties [20]–[24] is considered as the key to developing these two important industries. Indeed,

material technologies are regarded as the key development direction for each country if they want to build the industry. Among these, foam iron production technology provides the metallurgical industry with an advanced raw material with low carbon content and impurities. Due to this reason, foam iron-based steels have higher durability and ductility than cast and scrap steel. Fig. 1a shows structural steel grades classified according to strength limit and elongation [25]. Unlike conventional high-strength steels, which are strengthened by solid solution and dispersed phase secretion, advanced high-strength steels are strengthened by phase transformation and often contain ferrite, bainite, residual austenite, and possibly martensite, as shown in Fig. 1b [26].

These steels have high strength, and some have good ductility (suitable for forming), so they are widely and increasingly used. An increase in manufacturing structural details in the automobile industry, marine industry, and defense industry to meet technical and safety criteria. Among the advanced high-strength steel families, low Mn steels with

phase change due to plastic deformation are steel lines with high strength, ductility, and good fatigue resistance; they are very suitable for manufacturing load-bearing mechanical parts by the deformation process [27].

(a)
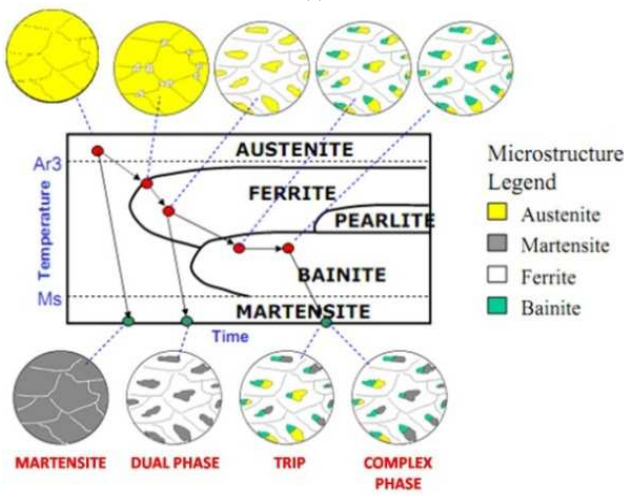
(b)

Fig. 1 a) Relationships between strength and elongation for some steel types [25], b) Thermal processing routes for AHSS [26]

The phase transformation effect due to plastic deformation was introduced by Zackay et al. [28] when studying the austenite transformation into martensite that appears during the deformation process of some types of stainless steel, as shown in Table I.

TABLE I
TRIP STEEL CHEMICAL PROPORTION [28]

C	Si	Mn	Cr	Ni	Mo
0,31	1,92	2,02	8,89	8,31	3,8
0,25	1,96	2,08	8,88	7,60	4,04
0,25	1,90	0,92	8,80	7,80	4,00
0,25	-	-	-	24,4	4,10
0,23	-	1,48	-	22,0	4,00
0,24	-	1,48	-	20,97	3,57

The special point is that the residual austenite in the structure of TRIP steel is rich in carbon and sensitive to deformation [27]. When subjected to plastic deformation, residual austenite will transform into martensite and become the challenging phase in the matrix, as shown in Fig. 2a. Thanks to that, this type of steel has both high ductility due to the initial residual austenite in the structure and high durability after plastic deformation due to the austenite

transforming into martensite. This type of steel has been and is being used to produce many details in the automotive and maritime industry and is expected to be one of the steel types of the future automotive industry, as shown in Fig. 2b.
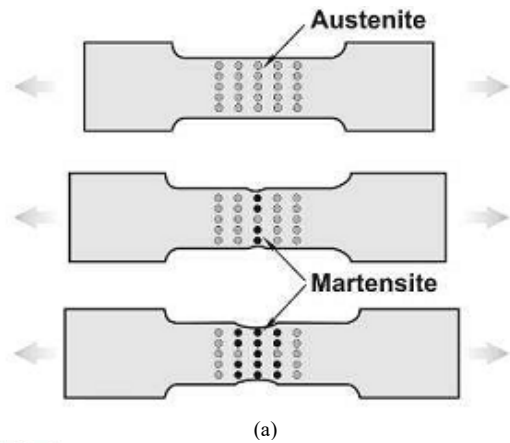
(a)

(b)

Fig. 2 a) Phase transformation in TRIP steel during tensile testing [28], b) Application of TRIP steel in industry [29]

TBF steels may be manufactured by a hot rolling process similar to other Advanced High Strength Steel (AHSS) grades. Hot-rolled transformation-induced plasticity (TRIP) steels offer some benefits compared to typical hot-rolled TRIP steels. Traditional TRIP steels consist of a polygonal ferrite matrix in their microstructure. The manipulation of multiphase microstructure is achieved by altering the cooling rate and duration following the hot rolling of austenite in several stages [30]. Producing high strength levels in ordinary TRIP steels is challenging because of the restricted quantities of carbon, manganese, and silicon. Past research has attempted to use other alloying elements to address this issue. Hashimoto and colleagues enhanced the tensile strength of TRIP steels by incorporating molybdenum and niobium [31]. The polygonal ferrite matrix causes low tensile strength and poor stretch-flange ability [32]. Hot-rolled TBF steels were designed to address these concerns. TBF steels, when hot-

rolled, need a simpler procedure than traditional TRIP steels to get a bainitic matrix that offers enhanced strength and increased ductility. Mn segregation bands and martensite/austenite islands develop following hot rolling [33]. Producing TRIP steel billets must go through two stages: the smelting and refining stage to create casting billets and the thermomechanical processing stage to create steel plate billets with proper structures [34]–[37]. In the world, most countries smelt steel from ore and then refined and mixed alloy elements. After casting, it will be thermo-mechanically processed according to the hot rolling or cold rolling process. However, this process makes the molded sample vulnerable to defects [37]–[41]. The second trend is to process continuous rolling casting equipment. However, this process is complex and requires advanced technology.

Due to their versatility and excellent formability, there is a high expectation that TRIP bainitic-supported ferrite TBF alloy steels and partition quenching steels will emerge as 3rd generation high-strength steels [42], [43]. The bainite transformation is recognized as a semi-diffusion phase transformation with the participation of a slip mechanism similar to the martensitic transformation and a diffusion mechanism, in which the slip mechanism preferentially occurs first [44]. In TBF steel, the initial bainite transformation product is C-supersaturated ferrite bainitic. A sliding mechanism and untransformed austenite form it because the sliding kinetics depend on the temperature gradient. When retaining heat, C will diffuse from the supersaturated bainitic ferrite to the surface of austenite to form a C-rich region. However, due to the presence of elements Si, Al... available in steel, the cementite secretion process has yet to occur because it takes time for these elements to diffuse from the cementite formation area [42], [45], [46]. Due to this reason, C continues to diffuse and enrich the untransformed austenite. Indeed, the kinetics of bainite transformation depend on many factors, including the proportion and chemical composition of austenite upon heating, temperature, and bainite retention time. Therefore, to control the proportion of residual bainite and an austenite phase, it is necessary not to maintain both the heating temperature and holding time and the isothermal cooling temperature and time [47]–[50]. Thus, this paper aims to comprehensively understand Bainite phase transformation and its mechanism in TBF steel.

II. MATERIALS AND METHOD

This paper aims to present a comprehensive understanding of the Bainite phase transformation mechanism in TBF steel. Thus, the relevant publications in the Scopus/Wos/Google Scholar database were carefully selected for review. Some criteria relating to inclusion and exclusion were used to ensure the quality and quantity of papers.

After reviewing these selected papers, three elements of C, Mn, and Si are the main ones that significantly affect the transformation mechanism in TBF steel [37], [42], [45], [51]–[54]. In addition, we found that the temperature and retention time in the heating process are important parameters. Indeed, to have the required low Mn steel structure, it is necessary to choose a quenching environment with a cooling rate more significant than the critical cooling rate when cooling the steel from the vital zone to the bainite zone. If the cooling rate is slow, it can lead to pearlite formation, reducing the proportion of residual bainite and austenite and leading to a reduction in the strength and ductility of the steel [42], [47], [55].

The two basic parameters of the isothermal cooling process are the temperature T_B and the heat retention time t_B in the bainite region [49], [56]–[58]. These two parameters control the ratio and solubility of C in the two phases, bainite and residual austenite. When the heat is kept too short, the untransformed austenite has a C content that is not rich enough for thermal stability. Therefore, when cooled to room temperature, they partially transform into carbon-saturated ferrite (martensite), causing the final residual austenite fraction to decrease. If the heat is kept too long, the untransformed austenite will be saturated with carbon, and it will quickly release cementite, causing the fraction and C content in the untransformed austenite to decrease, so the final fraction of residual austenite obtained is low. Therefore, an optimal holding time exists to obtain the maximum residual austenite fraction. Summarizing through some documents, this time value is in the range of 2-20 minutes. On the other hand, the fraction of untransformed austenite is low, while the diffusion of C takes place slowly, requiring a long time for the austenite to be rich enough in C for thermal stability. Therefore, the final residual austenite fraction is also low. Thus, an optimal temperature exists in the range of 350 - 450°C to receive the most significant proportion of residual austenite [59].

III. RESULTS AND DISCUSSION

A. Mechanism of TBF Transformation

1) Austenitization transformation

At room temperature, steel has a two-phase organization: ferrite and cementite. When heating steel to the temperature range between Ac_1 and Ac_3, the two-phase structure of ferrite and austenite will be obtained, as shown in Fig. 3. When steel is cold rolled before calcination, there will simultaneously be recrystallization of ferrite and the formation of austenite after calcination.

TBF steel transformation mechanism: Austenite formation includes two stages: nucleation and germination.

- Nucleation: In the crystallization theory, there are two forms of nucleation: independent nucleation and nucleation on an existing substrate. Many research projects have confirmed that austenite seeds mainly form at the Fe-cementite boundary because carbon accumulation is detected at the grain boundaries [48], [62]–[68].
- Germination: After being formed, the germ continues to grow to form austenite, although the newly formed austenite is not yet uniform in chemical composition [62], [65], [66], [69]–[73].

The austenite sprouts form in contact with cementite and ferrite. As the austenite grain grows, its boundaries move toward the ferrite and cementite. When first formed, because the carbon concentration in austenite is still low, the carbon in cementite will enter the austenite, causing its carbon concentration to increase. The boundary surface must grow toward the cementite to ensure equality at a given temperature. On the other hand, increasing the carbon concentration in austenite also unbalances the carbon

concentration at the ferrite-austenite interface [49], [50], [62], [65], [70], [74]–[76].
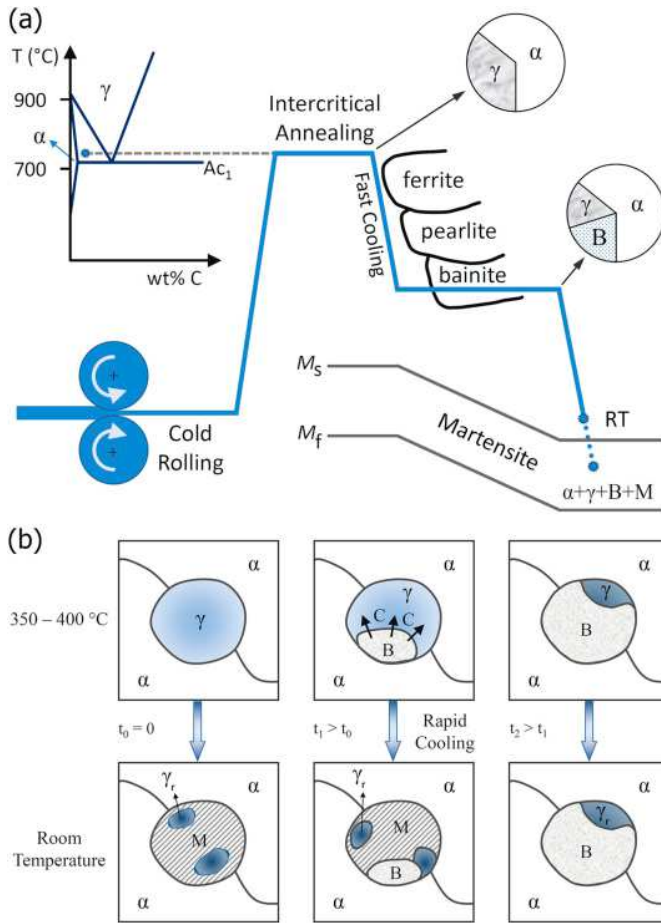

Fig. 3 a) Heat treatment of TRIP steel, b) the changes in the structure after IBT treatment [72], [73]

Factors affecting the transformation process are included as follows: Initial structure (for steels with fine structure, there will be a ferrite-cementite grain boundary, increasing the austenite transformation process); Carbon content (when carbon content increases, the conversion speed also increases); Alloying elements (must consider how alloying elements affect the stability of the carbide as well as the fineness of the carbide) [38], [53], [77], [78].

When studying the crystallization process from liquid, there are two nucleation mechanisms: autogenous nucleation and parasitic nucleation. The process of autogenous nucleation can only occur with an immaculate monolithic system, the nucleation at this time is only based on the energy and structural three-kinetic factors. Such a nucleation process is uniform nucleation, meaning that the probability of starting to encounter nucleation in the entire volume is the same [79]–[82]. Due to the appearance of preferential nucleation regions, an uneven nucleation mechanism is created with the parasitic nucleation process. It can be seen that the nucleation of new phases in solid phase transformation only exists in priority regions for nucleation of new phases because, in the crystal lattice of the solid phase, there are always different types of lattice defects. Indeed, various types of lattice defects always increase the system's free energy and thus favor three kinetic energies when nucleating new phases. In addition, it should

consider how each type of crystal lattice distortion affects the nucleation of new phases [83]–[90].

Fig. 4 illustrates the initial idea of cold-rolled TBF steels, which includes complete austenitization followed by rapid quenching to a temperature higher than the austempering stages, resulting in a microstructure with RA grains inside a bainitic matrix. In the partly austenitized TBF steel idea, a multiphase microstructure may be achieved with fine-grained ferrite and RA grains surrounded by bainitic islands [33]. At elevated intercritical temperatures, a decrease in the concentrations of carbon and manganese in the intercritical austenite is expected to cause a shift of the bainitic transformation curve to the left and higher temperatures. Consequently, it is necessary to elevate cooling rates and reduce the transformation period by raising the intercritical temperature to promote bainitic transition. An increase in Ms temperature was reported due to reduced quantities of C and Mn in intercritical austenite at higher intercritical temperatures [33].
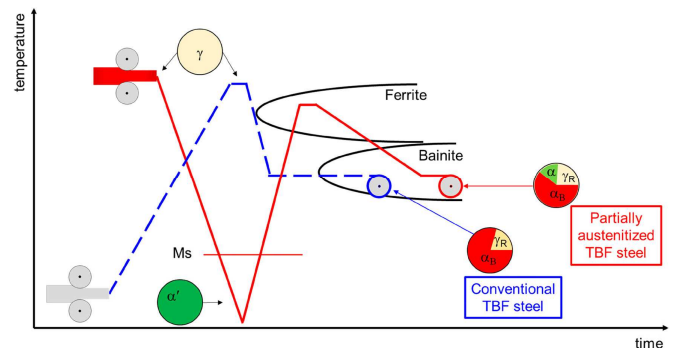

Fig. 4 Partial authentication and the conventional process in TBF steels [33]

2) Influence of phase interface structure on solid phase transformation:

When a new phase is formed within an original (parent phase) phase, a border will appear between the new and old phases (condition for phase stability). However, the phase interface has many different structural forms, specifically:

- Self-interstitial: It is a crystal lattice of two continuous phases; however, there is a change in the size of the lattice parameters, as shown in Fig. 5a. The characteristic of the crystal lattice structure is that the elastic energy is significant, and the surface energy is negligible. Thus, if the newly created phase has an inter-lattice structure, it will minimize the surface energy and, therefore, be easier to form (at the beginning of building a new phase) [48], [61], [89]–[91].
- Semi-coherent: The crystal lattice of the parent phase and the new phase has both a continuous and interrupted structure, as shown in Fig. 5b. Thus, the elastic energy will gradually decrease due to the compression of the two solid phases and the interruption of elastic waves in the crystal, while the surface energy will slowly increase due to the formed phase interface [48], [61], [90].
- In-coherent: It is a structure in which the newly formed phase has a separate lattice position from the parent phase, and the continuity of the crystal lattice is eliminated, as shown in Fig. 5c. At that time, the phase

interface reaches its maximum value and is stable. Therefore, the surface energy is the largest, and correspondingly the elastic energy is the most minor [48], [61], [62], [81], [90], [92], [93].

Thus, with the three structural types of the phase interface mentioned above, it can be seen that, when creating a new phase, the lattice parameters positioning the lattice direction are far different from the original parent phase, leading to very high surface energy. Therefore, to reduce surface energy, the new phase always connects with the parent phase. Because of this self-interstitial tendency, the crystal faces and directions, as well as the lattice parameters of the new phase, must have a definite correlation with the parent phase. The process continues with the growth of the latest phase accompanied by an increase in surface energy and a decrease in elastic energy. Therefore, in reality, many new phase formation processes must go through the intermediate stages of self-interstitial → semi-coherent→ in-coherent [48], [61], [62], [70], [75], [76], [94]–[96].
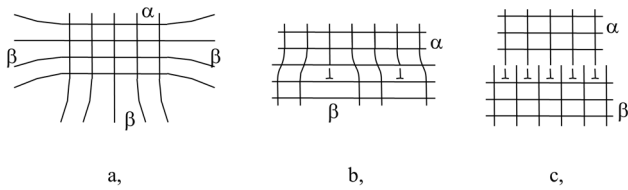

Fig. 5 Types of grain interface structures; a) Self-interstitial; b) Semi-coherent; c) In-coherent; α - Parent phase, β - New phase [90][48], [61]

3) Nucleation of new phase crystals on grain boundaries:

As mentioned, crystal grain boundaries are a form of lattice defects, so the grain boundaries themselves have high energy levels. Therefore, when nucleating a new phase on the grain boundary, part of the surface energy is lost to provide energy for the nucleation of the latest phase. On the other hand, for many-atom systems, grain boundaries are favorable places for creating the phenomenon of elemental composition of elements. Therefore, it is suitable for generating three-component kinetics, by the component concentrations of the new phase. With the above analysis, it can be seen that the grain boundary is one of the priority regions for new phase nucleation. The concentration of alloying elements on grain boundaries is explained as follows: alloying elements have size differences with solvent elements (atomic diameter, lattice parameters). Therefore, when these elements are secreted along grain boundaries, they will cause less disruption of the solvent crystal lattice. Experiments also show that alloying elements are mainly concentrated at grain boundaries. Quantitatively, the following formula can be used to calculate the alloy element content at grain boundaries [48], [56], [60], [70], [74], [95], [97]–[100]:

$$C_{Grain\ boundary} = \frac{C_0\ exp\left[\frac{E}{K.T}\right]}{1 + C_0\ exp\left[\frac{E}{K.T}\right]} \qquad (1)$$

Where:
C_o = Concentration of alloying element;
E = Energy difference when alloying elements dissolve in grains and grain boundaries;
K = Boltzmann constant;
T = Kelvin temperature (^{o}K).

Experiments also show some poor alloying elements on the grain boundaries. These elements are not concentrated on grain boundaries mainly due to chemical effects and electron-shell interactions between solute and solvent. Another important thing for the nucleation of new phases at grain boundaries is that the diffusion of substances at grain boundaries is relatively easy compared to diffusion within crystal grains. According to the experiment, the energy to activate the diffusion process at the grain boundary is only one-half that in the crystal grain, and the diffusion coefficient D on the grain boundary is about 1000 times compared to that in the grain. Therefore, it can be concluded that the grain boundary is a very favorable region for the formation of new phases [45], [80], [81], [84], [93], [101]–[103].

4) Nucleation of new phase crystals on the dislocation line:

When considering the dislocation model in the crystal, it can be seen that the crystal lattice is dislocated around the dislocation axis, which creates favorable conditions for the concentration of alloying elements along the dislocation axis, making the crystal lattice connection between the old phase and the new phase more accessible [79], [84], [86], [88], [102], [104]. At the same time, it can be seen that the dislocation line itself has energy, and therefore, when nucleating on the dislocation line, the dislocation will give up some of the energy to the nucleation work. Another feature is that along the Cottrell dislocation axis, there exists a high concentration of alloying elements, creating favorable conditions for the formation of new phases with high concentrations of alloying elements. The last thing is that when nucleating a new phase on a dislocation line, the growth of a new phase is more manageable because the ability of atoms to diffuse along the misaligned axis is more favorable, called the Tunen diffusion mechanism [49], [60], [61], [64], [70], [105], [106]. The diffusion activity along the dislocation axis is one-half compared to that in the grain, and the nucleation rate on the dislocation axis (N) is 10^{78} times that of autogenous nucleation. Thus, the deflection lines are also priority areas for creating new phases very powerfully and effectively.

5) Nucleation of new phase crystals on misaligned surfaces:

In crystals, defects always exist, including misaligned defects, which can change to an order of another lattice type. Therefore, if the newly created phase has a lattice type corresponding to the new order, it will be favorable for creating a new phase. When misaligned surfaces are formed, the atoms of the solutes tend to concentrate in the old phase transition zone. Misaligned surfaces create a Suzuki atmosphere, which is favorable for generating a new phase with high-concentration solutes. Besides, at the boundary of misaligned surfaces, incomplete dislocations ($|\vec{b}|<$ one lattice parameter) are formed, creating favorable conditions for nucleation. With the above characteristics of misaligned surfaces, this is also a priority area for new phase nucleation. This is especially meaningful when creating new phases of materials through plastic deformation due to the high degree of lattice dislocation for misaligned surfaces. This could be because the increased dislocation density results in many grain boundaries [86], [107]–[113].

6) Nucleation of new phase crystals on solid impurity particles:

In the crystal structure of a solid, solid impurities always exist. When solid impurity particles appear, if the new phase formed on the impurity particles will have a surface tension of γ, the surface tension between the latest phase and the old phase is γ. Therefore, creating new phases on solid impurity particles will be easier if γ' < γ (ie reducing surface energy), as shown in Fig. 6. On the other hand, because the thermal expansion coefficients of the solid impurity particles and the old phase are different, heat treatment on the interface between the base phase and impurities will create surface misalignment, which will create favorable conditions for nucleation. However, nucleation on solid impurity particles plays a secondary role because their length is too small compared to other defects.
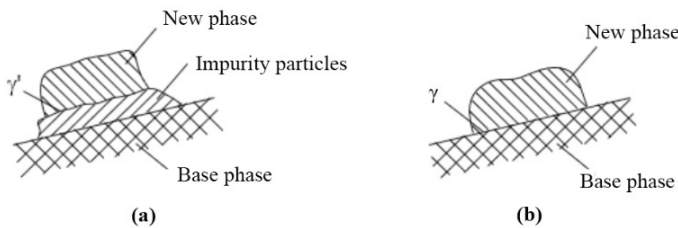

Fig. 6 Diagram of new phase nucleation on solid impurity particles ; a) γ' < γ : Nucleation on impurity particles; b) γ' > γ : Nucleation on base phase [48], [61], [90]

In addition, it can be seen that there always exist many microscopic undulations in the crystal, including the main types such as microbubbles, microcracks, and microbumpy that are formed a lot due to the slip process during plastic deformation. These microscopic undulations can exist on the outside or inside of the crystal. When microscopic undulations appear, they will have the prominent characteristic of causing breaks and fractures, causing loss of continuity of the elastic medium, and loosening the elastic field. Then, the germination of the new phase at the microscopic undulation will be generated more quickly because the elastic energy is negligible. However, in reality, the nucleation of new phases in solids does not follow only one mechanism. Still, it is always a combination because many different types of defects always exist in the crystal lattice. The problem is which mechanism plays the dominant role, resulting in a complete dependence on the initial state of the crystal types [45], [78], [118], [83], [90], [107], [111], [114]–[117].

7) Transformation of bainite and formation of residual austenite:

When cooling steel from the critical temperature zone to the bainite temperature zone, austenite will transform into different products, such as new ferrite, pearlite, bainite, and residual austenite, depending on the cooling rate. If the cooling rate V_c is greater than the critical cooling rate V_{cc}, no new ferrite and pearlite will form. When retaining heat, C will diffuse from C-saturated bainitic ferrite to the surface of austenite, forming a C-rich region. The C diffusion process stops when the C concentration in austenite reaches the

equilibrium line To, where the free energies of austenite and ferrite are equal, as shown in Fig.7.
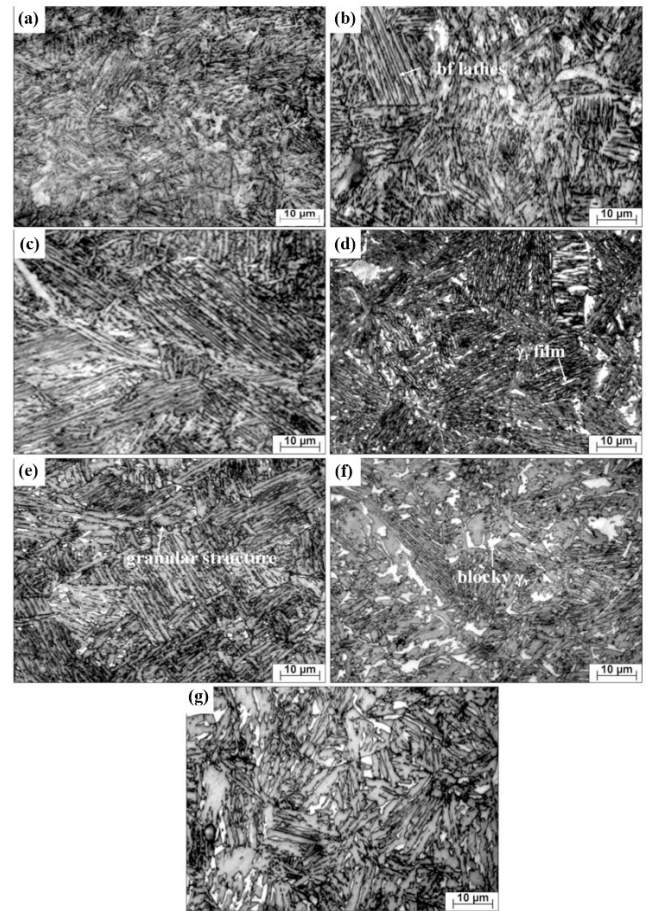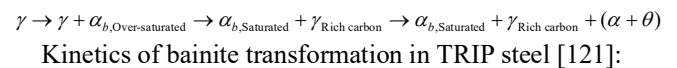

Fig. 7 Optical micrographs of the TBF steels austempered at; a) 325°C, b) 350°C, c) 375°C, d) 400°C, e) 425°C, f) 450 °C and g) 475°C for 20 min [119]

This leads to incomplete reaction; part of the austenite is retained even when kept in heat for a very long time. Thus, the bainite transformation process can be briefly described as follows: [37], [42], [114], [120], [80]–[83], [85], [92], [93], [102]:

$$\gamma \rightarrow \gamma + \alpha_{b,\text{Over-saturated}} \rightarrow \alpha_{b,\text{Saturated}} + \gamma_{\text{Rich carbon}} \rightarrow \alpha_{b,\text{Saturated}} + \gamma_{\text{Rich carbon}} + (\alpha + \theta)$$

Kinetics of bainite transformation in TRIP steel [121]:

$$\frac{df_{\alpha_b}}{dt} = \frac{u.k_1}{f_{\alpha_b}^*}.(1 - f_{\alpha_b}).(1 + \beta.f_{\alpha_b}^*.f_{\alpha_b}).\exp[\frac{k_2(\Delta G_m^0 - G_N)}{rRT}.f_{\alpha_b} - \frac{k_2}{RT}(1 + \frac{\Delta G_m^0}{r})]$$

According to Fu and colleagues [39], residual austenite in TBF steel is a C-rich phase (about (0.6% - 1.8% C). Therefore, it has high durability thanks to the stabilizing effect of the solid solution of C and the high content of Mn and Si elements (about 1% - 2%). According to the law of mixing phases, for TBF steel to have high durability, the strength of the ferrite base phase must be increased. According to the principle of dislocation braking, it is possible to introduce some soluble elements of small enough size into the α -Fe lattice to improve stability. Based on the chemical element's universality, TBF steel contains C elements in interleaved soluble forms and Mn and Si in alternative soluble forms [122]. Moreover, elements such as Nb and Ti could be added to TBF steel, aiming to act as modifiers to generate small and fine ferrite particles by

forming solid compounds NbC, NbN, TiC, and TiN with petite sizes (< 400 nm), scattered in the ferrite matrix, hindering grain growth [123]. However, according to some studies, Nb has the effect of increasing the durability and maintaining ductility of TBF steel. Indeed, adding Ti strongly increases durability and decreases elongation significantly. The reason is that Ti interacts strongly with C, causing the loss of C in austenite in the critical region and, at the same time, accelerating the transformation of bainite, thus reducing the proportion of residual austenite in the steel, reducing elongation. Meanwhile, Nb has the opposite effect [124], [125].

8) Characteristics of the bainite transformation:

In terms of structure, bainite is similar to perlite, which is a eutectoid mixture of two phases of ferrite and carbide. However, there is a difference in the structure of the two phases. In perlite, cementite exists as parallel plates interspersed in ferrite. In bainite, cementite does not exist in sheet form but is usually in rod shape with tiny size and very high dispersion. Ferrite in bainite also exists in the form of fine needles. Bainite is divided into two forms: upper bainite (when cooled in the range of 500 - 350°C) and lower bainite (when cooled in the range of austenite (350 - MS) $^\circ$C. With upper bainite, the ferrite needles are in the form of clusters, and cementite is in the form of fine rods distributed on the contact surface of the ferrite needles, as shown in Fig. 8a. In the lower Bainite, the Ferrite needles merge to form 60°, rod-shaped cementite is distributed at the edge of the ferrite needles, as shown in Fig. 8b.
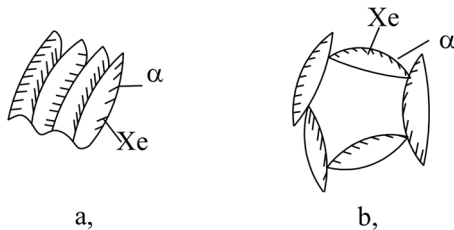

Fig. 8 Structure of bainite; a) Upper bainite, b) Lower bainite [45], [90], [126]

The structure of the phases in bainite also has characteristics that are different from those in pearlite. Cementite in bainite is essentially just K(ε) type carbide with the formula $Fe_{2.4}C$; this is a type of carbide that is not as stable as cementite (Fe_3C). Ferrite in bainite structure is a supersaturated solid solution, unlike pearlite, which is in an equilibrium or near-equilibrium state. Thus, if comparing bainite and martensite, the upper bainite has a structure similar to martensite, while the lower bainite has a structure identical to tempered martensite. The crystallographic relationship between bainite and austenite is very similar to that between martensite and austenite. For example, in lower bainite, the $(111)_\gamma$ surface is parallel to the $(110)_\alpha$ surface. The $[110]_\gamma$ direction parallels the $[111]_\alpha$ direction. In upper bainite, the $(111)_\gamma$ surface is parallel to the $(110)_\alpha$ surface and the $[211]_\gamma$ direction is parallel to the $[110]_\alpha$ direction. In medium carbon steels, the boundary between upper bainite and lower bainite is usually 350°C. This boundary is not fixed but changes according to the carbon content in the steel, as shown in Fig. 9 [48], [60], [127], [61], [68], [69], [94], [107], [112], [114], [115].
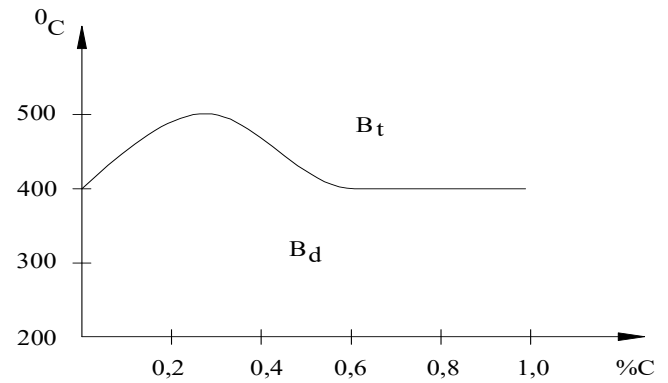

Fig. 9 The dependence of the upper Bainite and lower Bainite boundaries on %C [48], [61], [90]

Fig. 10 shows a comprehensive low-magnification TEM picture of the tested TBF specimens. The T-350 sample has a distinctive parallel arrangement of bainite laths with a small width of 100 to 200 nm, contrasting with the blocky bainite structure shown in the T-450 sample. The size and shape of RA undergo substantial alterations. RA is equally distributed throughout the bainite laths in the T-350 sample, displaying a dominating film-like structure with a narrow width and an average size of 30–50 nm, as shown in Fig. 10a. This result suggests that RA stability decreases as IBT temperature increases [128].
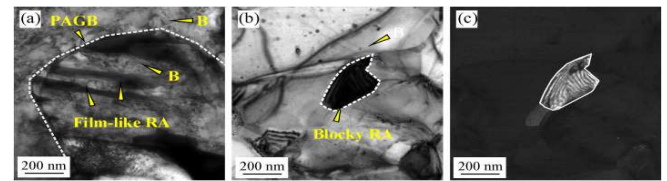

Fig. 10 TEM micrographs of typical samples [128]

9) Bainite transformation mechanism:

Bainite transformation occurs at temperatures less than 500°C. Thus, the bainite transformation temperature is lower than the recrystallization temperature of iron. Therefore, in this temperature range, the diffusion ability of iron could be better. However, due to the more significant transformation temperature (200 - 250) $^\circ$C, the diffusion ability of carbon is still very high, and therefore, the diffusion coefficient of carbon in austenite is large D_γ^C. The mechanism of Bainite transformation includes two fundamental processes: the transformation of the crystal lattice from the face-centered cubic of austenite to the body-centered cubic of ferrite and the process of redistributing the carbon concentration and excreting carbide [36], [43], [132], [66], [76], [78], [87], [88], [129]–[131].

The crystal lattice transition from γ to α is carried out according to the lattice slip mechanism, such as martensitic transformation. Experimental studies have clearly shown that bainite transformation also creates ridges on the flat sample surface, which confirms the presence of lattice slippage. On the other hand, in some types of steel, especially low alloy steels, bainite transformation is an incomplete transformation because there always exists a residual amount of austenite,

315

and the crystallographic relationship between bainite and austenite is very close; it is the same as the martensitic transformation. The implementation of the lattice slip mechanism is explained by the fact that the transformation temperature is lower than the recrystallization temperature of iron; the diffusion coefficient of iron is very weak, so redistribution of Fe atoms must not be carried out. However, there is a problem that lattice slippage occurs at temperatures greater than MS [75], [99], [100], [133], [134]. This explains that the transformation occurs at higher temperatures (200 - 250) ℃, and the diffusion ability of carbon is quite large. Due to the effect of diffusion, within the volume of martensite, there are always active regions of carbon content. In carbon-poor areas, the beginning temperature of the MS martensite transformation increases. If the Bainite transformation occurs, γ will form α similar to the martensitic transformation (lattice

slip mechanism). Such a sliding process only continues in carbon-poor regions, and therefore, the rate of formation of α from γ depends on the diffusion ability of carbon, leading to the difference between the bainite transformation and the martensitic transformation in terms of the slow rate of transformation and the Bainite transformation occurs gradually. The α needles produced have an oversaturated carbon concentration, and the diffusion ability of Fe is poor, leading to the secretion of carbide to reduce the carbon content. In areas rich in carbon, cementite nucleation is favorable. When cementite seeds develop, the surrounding areas will become poor in carbon, creating favorable conditions for the lattice slip process, leading to the formation of Bainite needles [34], [45], [138]–[140], [51], [52], [56], [76], [130], [135]–[137]. According to Entin, we have the following bainite transformation model, as shown in Fig. 11.
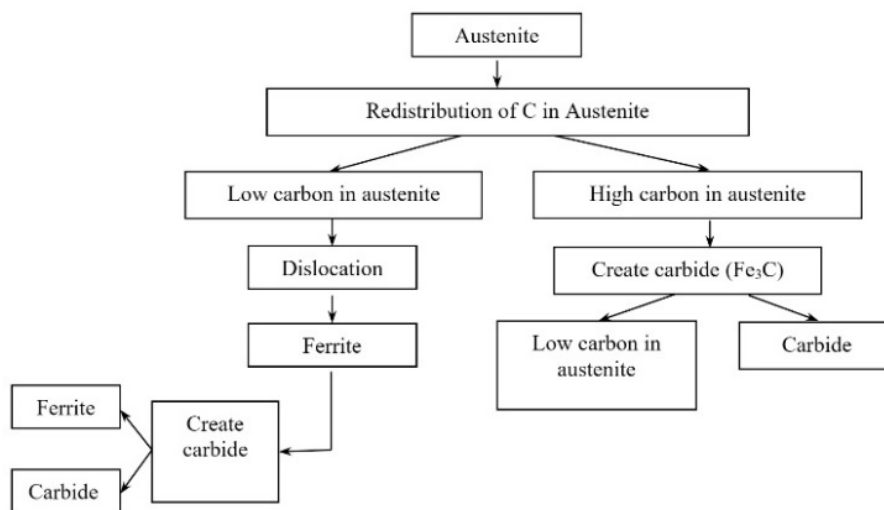

Fig. 11 Bainite transformation mechanism model [22], [48], [73], [100], [103]

In the above bainite, carbide is secreted along the ferrite needle border due to the high transformation temperature and high diffusion ability of carbon. In lower bainite, due to low temperature, the diffusion ability of carbon is reduced, so carbide is secreted right into the ferrite needle.

10) Bainite transformation kinetics:

Like pearlite transformation, the kinetic curve of bainite transformation also has a "C" shape. When isothermally cooled in the range of (530 - 470)℃, a mixture of fine pearlite and bainite is obtained. Thus, in this temperature range, the "C" curves of pearlite and bainite overlap. Cooled isothermally at a temperature less than 400℃, bainite without pearlite is completely obtained. With alloy steels, the alloying elements have the effect of splitting the kinetic curve into separate pearlite and bainite transformations and thus obtaining the austenite stability region. Bainite transformation can occur both through isothermal cooling and continuous cooling. However, the bainite transformation is incomplete but has a certain amount of residual austenite; the amount of residual austenite is even more evident with alloy steels. Bainite formation during the continuous cooling process also starts from a B_S temperature and ends at a specific B_f temperature, similar to the martensitic transformation. If you continue to cool the excess austenite after the transformation,

there will be a martensitic transformation (when the temperature is lower than M_S), then a mixture of bainite and martensite will be obtained) [38], [40], [83], [84], [90], [101], [116], [139], [141].

11) Martensite transformation under mechanical load:

When Austenite is rapidly cooled below temperature Ms, there will be a transformation into martensite. In terms of energy, it is due to the difference in free energy between the two phases.

- Martensite transformation due to stress (Ms to M_s^{σ}): Fig. 12 shows that the stress applied to austenite to transform into martensite is less than its yield limit, meaning the austenite is deforming elastically. The pre-existing martensite crystal nuclei in austenite will initiate the transformation in this temperature range. Therefore, martensitic transformation in this region is called martensitic transformation due to stress.

- Martensite transformation due to plastic deformation (M_s^{σ} to M_s^{ε}): Fig. 12 shows that the stress applied to austenite to transform into martensite exceeds its yield limit, meaning the austenite has deformed plastically. The mechanical force required to cause enough stress for transformation must be significant because the free energy between austenite and martensite is small. Austenite has deformed plastically, and at a certain deformation level, there will be shear bands

intersecting to nucleate the martensitic transformation. Therefore, martensitic transformation in this region is called martensitic transformation due to plastic deformation. However, no changes occurred at temperatures greater than Ms.
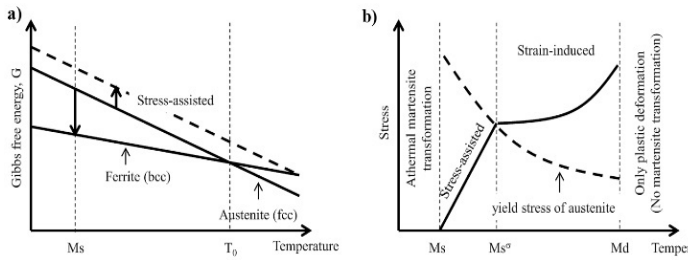

Fig. 12 Relationship between stress-assisted and strain-induced martensite [142]

Under certain conditions, residual austenite can transform into martensite when subjected to mechanical loading. When martensitic transformation occurs, there will be volume expansion and change in crystal lattice shape, causing plastic deformation called TBF deformation. Therefore, the surrounding area (ferrite, bainite, or residual austenite) is also deformed plastically based on ensuring deformation compatibility. In general, increasing the proportion of solid phase bainite and residual austenite will tend to strengthen enormously, increasing the durability of TBF steel. However, if the solid phase fraction is too large, the base phase will be hardened too vigorously, which can cause failure at a trim deformation level. Therefore, the phase fraction is an essential organizational characteristic of TBF steel and can be controlled by controlling the heat treatment parameters. In summary, the TBF effect is a special effect as an additional strengthening and deformation mechanism in TBF steel. To increase the strength and ductility of TBF steel, it is necessary to create a certain proportion of residual austenite phase to promote the role of the TBF effect [42], [45], [118], [138], [143], [144], [80], [81], [83], [87], [92], [93], [102], [104].

12) Start temperature of bainite transformation:

Various efforts have been undertaken to model-predict the bainite initiation temperature, with some advocating for a primary empirical method and others opting for a more advanced technique. Bodnar and colleagues [47] assessed the Bs temperatures of three steels characterized by high Nickel and Chromium levels and low Carbon content. They conducted a linear regression analysis based on a linear composition dependence. The contributions that emerged were indicative of the narrow scope of their research. Zhao et al. [62] conducted a linear regression analysis in a broader set of alloys, 82 obtained via Isothermal Transformation diagrams, making the results more widely applicable. Some writers considered the impact of earlier austenite particle size and cooling rate in addition to chemical composition [145], [146]. Some advocated non-linear dependencies, including exponential or polynomial composition relationships [127]. Mateo et al. [57] acknowledged the limitations of insufficient input data and chose to utilize a neural network model. Furthermore, there needs to be an indication about the importance of the factors or the weighting. The current method for defining initial temperatures relies on a basic statistical technique with a clear interpretation of parameters. The approach used linear regression analysis to establish a correlation between the material's temperature and the alloy's chemical composition to assess the impact of each alloying element. The current research used a structured and methodical methodology due to the significant effect of the individual alloys employed on the results of temperature experiments and the limited generalizability of the findings to other alloy data. The study was conducted sequentially on specific data sets, focusing on isolating the impact of each aspect as well as feasible. Alloying elements such as Mo, Cr, Mn, Ni, or Si were evaluated using linear regression analysis on ternary alloy data, with the two parameters for carbon held constant in each study. The unified equation results from analyzing the five Fe-C-M systems, using the fixed carbon parameter and intercept. The final equation combines all the coefficients produced [37], [42], [45], [51], [55], [78], [118], [131], [138].

$$WB_s(^oC) = 850 - 206C - 78Mn - 33Ni \\ - 70Cr - 75Mo - 61Si \quad (2)$$

C has the most significant impact on Bs temperature, followed by Mn and Mo, as shown by the equation. When utilizing a linear equation, it is assumed that there is no interaction between the alloying constituents. Furthermore, in the analyzed ternary systems, an indicator of this impact would be the discrepancy between the slope of the data and the projected line for the same composition. While most people agreed with the data, some data sets tended towards a steeper slope, suggesting a more significant carbon reliance in the Fe-C data and a potential interaction impact. However, a more rigorous examination would need higher-quality data.

Three potential approaches were initially available. First, a linear regression analysis is conducted with the C coefficient held constant while concurrently optimizing Mn and Si. The second analysis involves optimizing just Si while keeping the other factors constant, while the third analysis involves optimizing all three elements concurrently. Three equations were derived consequently [37], [42], [45], [51], [55], [78], [118], [131], [138]:

$$B_s = 850,44 - 206,15C - 81,79Mn - 57,61Si \quad (3)$$

$$B_s = 850,44 - 206,15C - 78,04Mn - 61,04Si \quad (4)$$

$$B_s = 833 - 241C - 74Mn - 36Si \quad (5)$$

when C is held constant in Eq. (3) and Eq. (4), there is a slight variation in the coefficients for Mn, which is much more negligible for Si. When all three components are optimized, the coefficient for Si in Eq. (5) is almost half of the previous values.

B. Mechanical Properties of TBF Steel

Regarding durability, the durability limit of bainite is greater than that of martensite because the ferrite needle is small, the carbide is highly dispersed, and the ferrite solid solution has a larger oversaturation. Particle size affects durability according to the Hall - Peten relationship [107], [110], [114], [115], [126], [147], [148].

$$\delta = \delta_0 + K.d^{1/2} \quad (6)$$

317

For the upper bainite, the carbide is dispersed on the grain boundaries, so the effect of hindering dislocation movement is reduced, and the toughening efficiency is low. For the lower bainite, the carbide is dispersed in the upper Ferrite needle, the deflection resistance is thus better, leading to more substantial dissolution, and the toughening efficiency is high. Therefore, the durability of Bainite gradually increases as the transformation temperature becomes smaller [99], [130]. Regarding the plasticity of bainite, it is more complicated than perlite. For the upper bainite, the carbide is dispersed on the needle surface because the ferrite needle is large, so the brittleness increases while the ductility is lower than that of pearlite. For the lower bainite, the ferrite needle is tiny and fine; the carbide is dispersed in the ferrite needle, so the plasticity increases, as shown in Fig. 13.
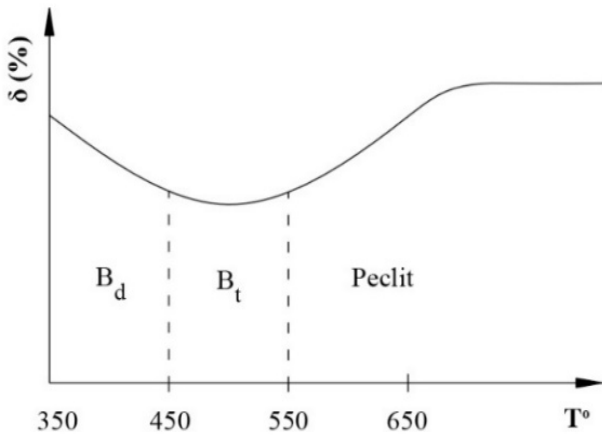

Fig. 13 Change in relative elongation of Perlite and Bainite [48], [57], [61], [76], [100], [149]

1) Carbon: C mainly controls the ratio and solubility distribution in each phase. The relationship between the carbon content in austenite (C_γ^{IA}) with the initial carbon content (C_o), ferrite fraction (f_α), and carbon content in ferrite (C_α) is determined according to Eq. (7):

$$C_\gamma^{IA} = \frac{C_0 - f_\alpha C_\alpha}{1 - f_\alpha} \qquad (7)$$

The C content in residual austenite depends on the temperature and time of bainite isothermal treatment (Fig. 14). Thus, the proportion of residual austenite depends on the initial carbon content C_o, temperature, and calcination time. The C content in Mn steel is low (0.1% - 0.4%). When the C content is below 0.1%, the residual austenite ratio is not large enough to promote the TRIP effect, and the durability of the steel is low. However, when the C content is above 0.4%, the proportion of the ferrite phase is low, eliminating the role of the base phase, leading to reduced ductility of steel.
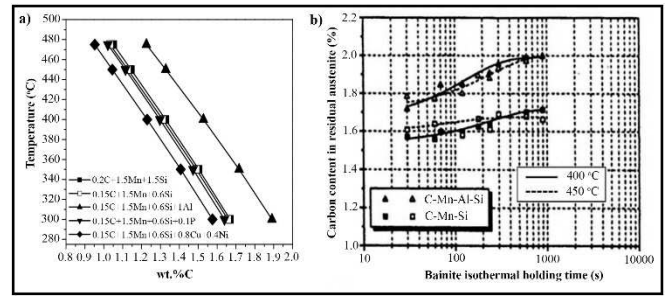

Fig. 14 Influence of Si, Al, P and Cu on the maximum enrichment of carbon in the austenite [34][150]

2) Manganese: The most critical effect of Mn is to increase the stability of residual austenite, making residual austenite exist at room temperature and, at the same time, increasing the hardness and durability of the phases (ferrite, bainite, residual austenite) due to the effect of stabilizing solid solutions. The Mn content in low Mn steel ranges from (1% - 2.5%). When the Mn content is <1%, the residual austenite is less stable, causing the low final residual austenite ratio and the low synthetic mechanical properties of the steel. Increasing the Mn content, the stability of austenite when calcined increases, and the transformation of austenite into bainite occurs more slowly, allowing C to have enough time to diffuse to enrich the residual austenite, thereby increasing the proportion of residual austenite and the degree of its stability [37], [43], [45], [55], [78], [138], [151].

3) Silica: The Si content in Mn steel should be as low as 1% - 2.2%. When the Si content is lower than 1%, the effectiveness of preventing carbide secretion is poor, the austenite becomes less stable, and the strength and ductility of the steel are low. Increasing the Si content could increase the proportion of residual austenite and its stability, the durability limit and mechanical properties of TBF steel, and the cold hardening and durability coefficient R_m/R_p. However, the Si content needs to be less than 2.2% due to the adverse effects of Si on steel such as reducing weldability, and the negative impact on the surface quality of steel when hot-rolled due to the formation of a tough FeO/Fe_2SiO_4 complex oxide film that makes it difficult to clean the surface [152]. In addition, Si also makes austenite particles smaller when calcined, helping to form a small, uniform second-phase structure, thus increasing durability and ductility [153][154].

Fig. 15 displays the standard mechanical parameters of tensile samples. All stress-strain curves in Fig. 15a show continuous yielding behavior without clear yield spots. As the IBT temperature rises in TBF samples, the yield strength increases from 602 MPa to 1180 MPa. The elongation first rises between 350–400 °C and after those declines. This is due to the existence of inter-critical ferrite. An increased IBT temperature leads to more excellent work-hardening rates due to the rising proportion of RA, as seen in Fig. 15b. Simultaneously, the work-hardening rate falls progressively as the real strain rises in all samples, suggesting a decrease in plastic deformability [128]. In addition, Fig. 16 shows typically elongated microstructures and microvoids in the sheared affected zone. Indeed, due to severe deformation, the bainite phases at 350°C exhibit greater elongation and thickness direction.
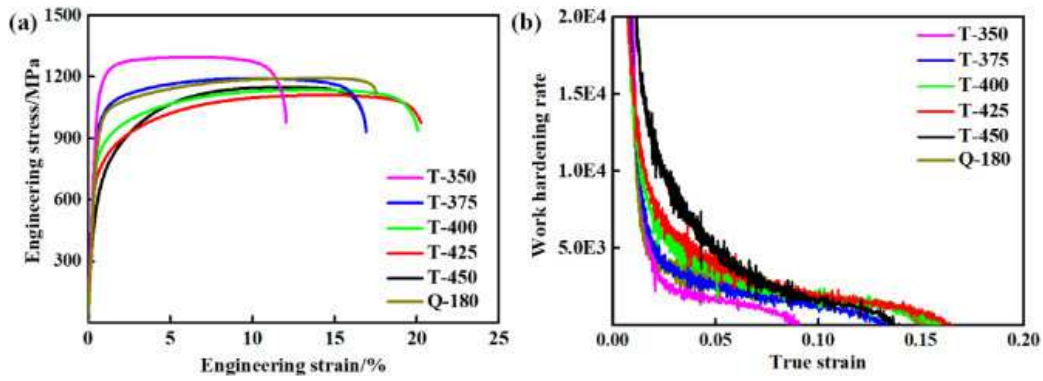
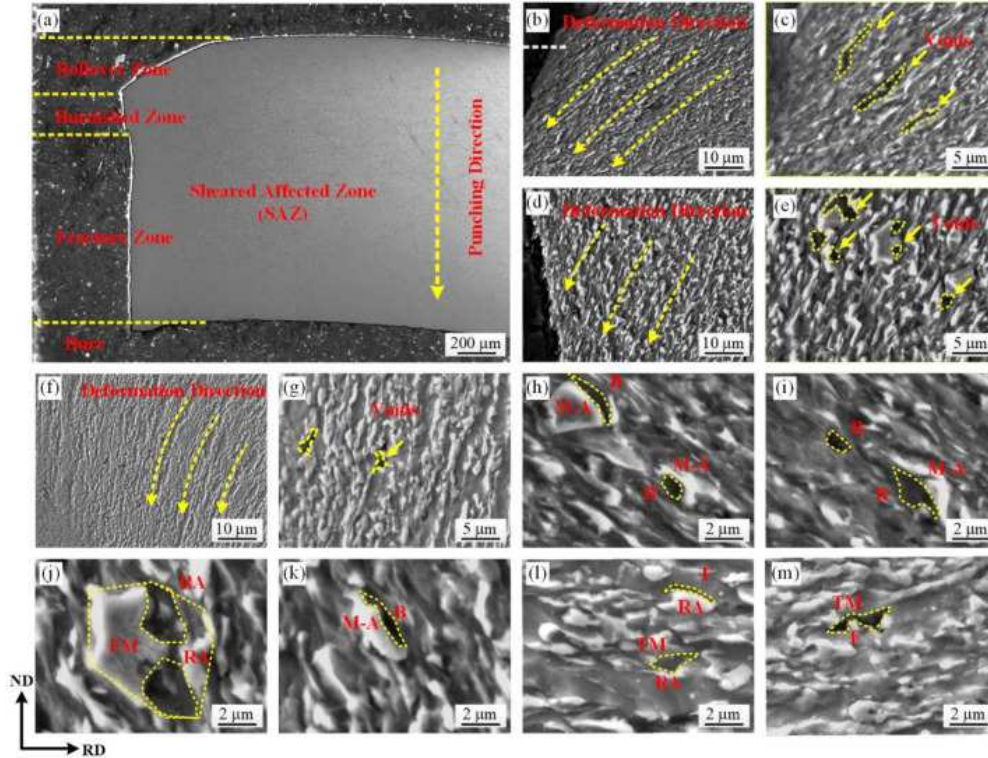Fig. 15 Mechanical properties of tested specimens [128]

Fig. 16 Secondary electron images of the punched specimens [128]

In the study by Nguyen et al. [155], they presented heat treatment of low Mn steel. The steel is heated to austenite temperature, holding the heat at a particular time to ensure a uniform process. Then, the steel is cooled to the Bainite transformation zone, retaining appropriate heat to obtain a three-phase structure of Ferrite, Bainite, and Austenite.

Finally, the steel is quenched in water to prevent austenitic degradation. After heat treatment, the results show that fine grain size is obtained with light and dark phases, which demonstrates the microstructure consisting of ferrite and austenite. Moreover, the mechanical properties of steel before and after heat treatment can be given in Table II.

TABLE II
MECHANICAL PROPERTIES OF TBF STEEL

Chemical composition	Phase percentage (%)			Mechanical properties				Ref
	Ferit	Bainite	Residue austenite	Rp (MPa)	Rm (MPa)	A (%)	RmxA (MPa%)	
0.1C-1.5Mn-1.5Si-0.5Cu	50	↓	↑ (≤3-11)	↓	↑	↑	↑	[156]
0.14C-1.5Mn-1.5Si-0.5Cu	50	↓	↑ (≤3-14)	*	↑	↑	↑	[156]
0.4C-1.5Si-0.8Mn	↑	↓	↑	-	↓	↑	↑	[157]
0.2C-1.44Mn-1.32Si	-	↓	↑ (6.3-13.5)	-	↓	↑ (31-41)	↑	[77]
0.18C-1.47Mn-1.8Si-0.28Al	↑	↓	↑ (6.5-16)	↑ (606-658)	↓ (967-940)	↑ (15-24)	↑	[158]

The impact of averaging temperature (400-450°C) and time in the bainitic range on microstructure and mechanical properties was examined in annealing simulations using two different cooling rates (30K/s and 50K/s) based on accurate continuous annealing line layouts (III), as illustrated in Fig. 17(a-c). Higher cooling rates result in marginally improved yield and tensile strengths, but lower uniform elongation values compared to lower cooling rates, as shown in Fig.17

(a-b). Quicker cooling reduces pro-eutectoid ferrite and bainitic ferrite formation during the cooling process. The highest level of consistent elongation is seen at every averaging temperature. Increased retention of austenite at room temperature leads to greater levels of uniform elongation. The stability of retained austenite is influenced by chemical stabilizations resulting from an optimal carbon content in austenite and a size effect [159].
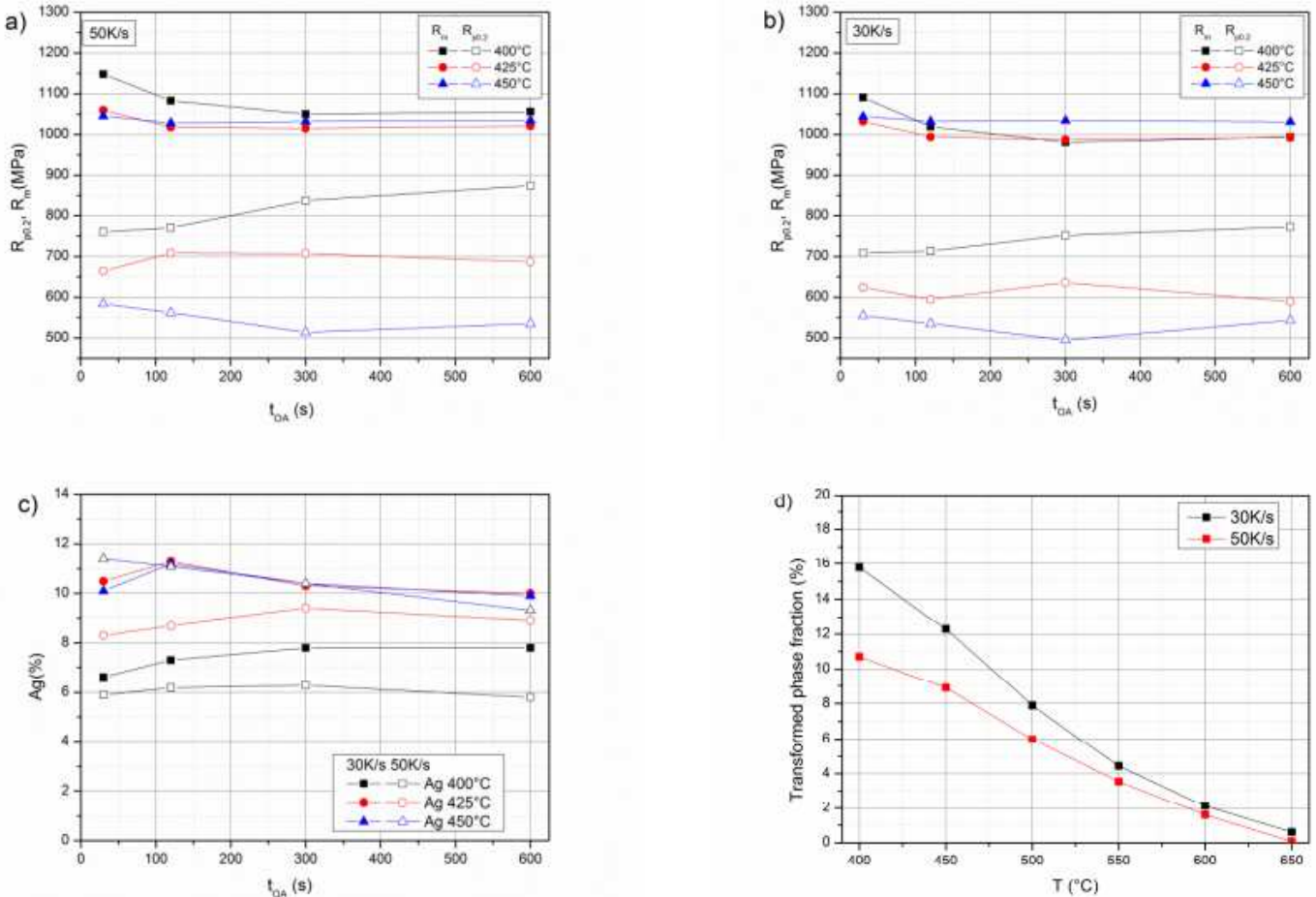

Fig. 17 a-c) Effects of the averaging temperature and time and cooling rate on mechanical properties [159]

The low carbon level in TBF steels may induce blocky austenite grains to convert into fresh martensite, encouraging the creation of M/A islands. Banding may impact the mechanical characteristics and fracture behavior in this scenario. Hot-rolled TBF steels are not as extensively researched as ordinary hot-rolled TRIP steels, despite the potential for enhanced mechanical qualities [33]. Chen et al. [160] achieved an ultimate tensile strength of 1219 MPa and a total elongation of 21% using a new steel alloy containing 0.21% carbon, 2.04% manganese, 1.04% silicon, 1.10% aluminum, 0.064% niobium, and 0.2% molybdenum. They achieved a granular bainitic matrix using final rolling at 890°C. However, dynamic strain-induced ferrite was identified from a microstructural perspective in relation to the final rolling temperature. In a recent study by Qian et al. [161], a bainitic matrix can be achieved in TRIP steel with the composition 0.28C–1.96Mn–1.62Cr–0.67Si–1.19Al–0.34 Ni–0.23Mo by using Austenite reversion transformation annealing during intercritical annealing, followed by long-duration isothermal bainitic treatment at 320°C for 2 hours.

They achieved an ultimate tensile strength of 1 GigaPascal and a total elongation of 29% after intercritical annealing of the martensitic starting microstructure.

Fig. 18a displays the stress-strain curves of partly austenitized TBF730, TBF770, and TBF800 steels. Fig. 18b shows how the yield strength (YS), ultimate tensile strength (UTS), uniform elongation (Ag), TE, and the product of UTS and total elongation (PSE) vary according to the intercritical annealing temperature. An inverse relationship is seen in the YS as the inter critical temperature rises. This tendency is due to the rising levels of RA triggering the TRIP effect when samples deform [33]. Fig. 19 compares the Ultimate Tensile Strength (UTS) and Total Elongation (TE) of the TBF steels tested in this research with those of TAM and TBF steels found in previous literature. The TBF730 steel has reduced mechanical characteristics because of a low intercritical temperature. Partial austenitization at 730°C results in decreased mechanical characteristics in TBF770 and TBF800 steels due to variables including the absence of residual

austenite and the presence of carbides at a lower intercritical temperature, unlike in other scenarios [33].
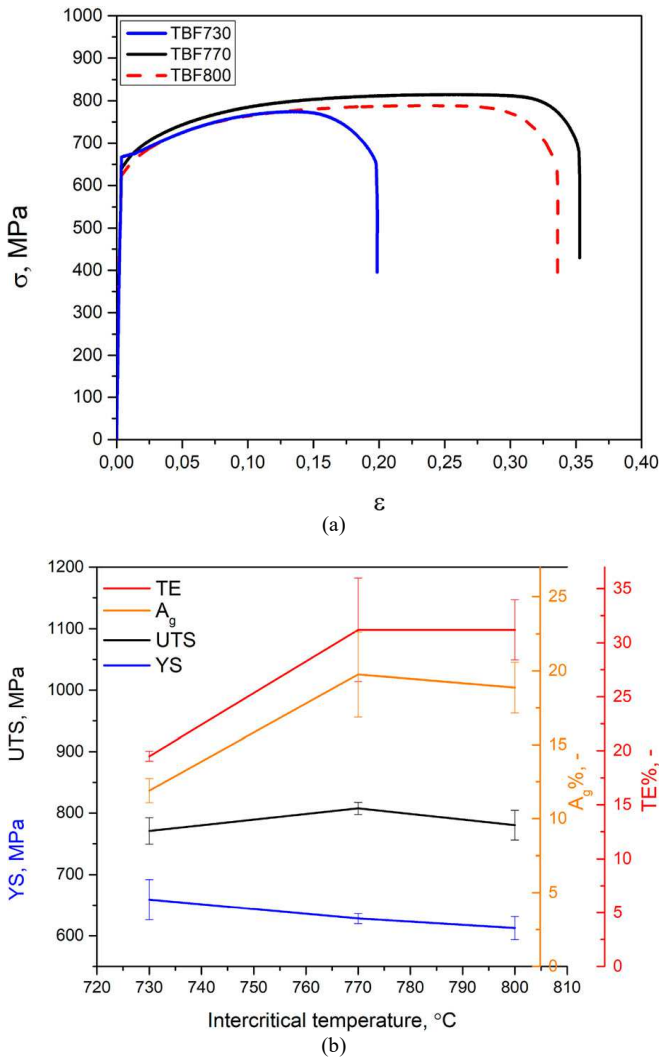

(a)

(b)

Fig. 18 a) Changes in engineering flow due to partial austenitization in TBF steels; b) Mechanical properties of TBF steel in case of partial austenitization [33]
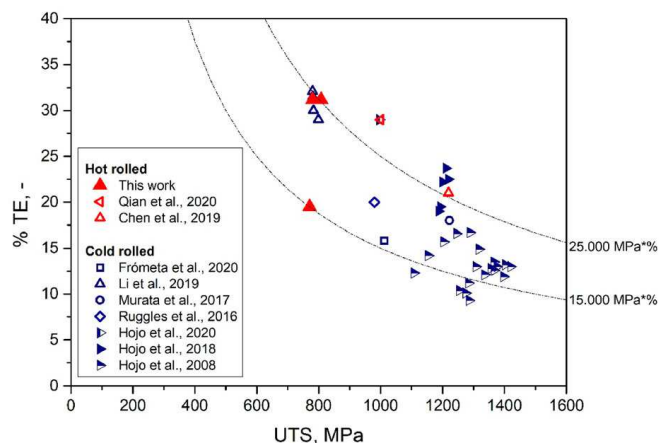

Fig. 19 Total elongation and tensile strength of TBF and TAM steels [33], [160]–[168]

IV. CONCLUSION

The article has presented the phase transformation mechanism, especially the bainite phase transformation for TRIP steel. The article also overviews the relationship between bainite transformation temperature and the composition of the studied steel. Thermodynamic analysis of TBF steel has also been reviewed and determined. The influence of alloying elements on the transformation mechanism and thermodynamics of TBF steel has also been studied and presented in this article. Overall, the general analysis of low Mn steels has been analyzed and presented in this work. Research results have shown the role of deformation and heat treatment in the stabilization of low Mn steel, as well as the influence of phases on the structure and properties of steel. The article has presented general research results on phase transformation theory and phase characteristics. Besides, the role of phases in steel durability is also analyzed. The following studies will also analyze the optimal heat treatment process, the interaction between phases, the mechanism of phase formation during deformation and heat treatment, and the role of deformation in strengthening steel. The article also analyzed and showed the structural forms formed after deformation and heat treatment for TBF steel. The article also analyzed and showed the influence of microstructure on the mechanical properties of researched steel.

REFERENCES

[1] P. C. L. Le, J. I. Kim, and K. Kim, "The growth of Korean companies and their contributions to the miracle of the Han River," *Int. J. Multimed. Ubiquitous Eng.*, vol. 11, no. 5, pp. 253–266, 2016.

[2] R. Yin, *Metallurgical process engineering*. Springer Science & Business Media, 2011.

[3] M. Ziółkowski and T. Dyl, "Possible applications of additive manufacturing technologies in shipbuilding: A review," *Machines*, vol. 8, no. 4, p. 84, 2020.

[4] T. N. Le, M. K. Pham, A. T. Hoang, T. N. M. Bui, and D. N. Nguyen, "Microstructure Change For Multi-Pass Welding Between Austenitic Stainless Steel And Carbon Steel," *J. Mech. Eng. Res. Dev.*, vol. 2, no. 2, pp. 97–102, 2018, doi: 10.26480/jmerd.02.2018.97.102.

[5] H. Anh Tuan, D. Nam Nguyen, and V. Viet Pham, "Heat Treatment Furnace For Improving The Weld Mechanical Properties: Design and Fabrication," *Int. J. Mech. Eng. Technol. (IJMET*, vol. 9, no. 6, pp. 496–506, 2018.

[6] T. N. Le, M. K. Pham, A. T. Hoang, and D. N. Nguyen, "Microstructures And Elements Distribution In The Transition Zone Of Carbon Steel And Stainless Steel Welds," *J. Mech. Eng. Res. Dev.*, vol. 41, no. 3, pp. 27–31, Sep. 2018, doi:10.26480/jmerd.03.2018.27.31.

[7] A. T. Hoang, V. V Le, A. X. Nguyen, and D. N. Nguyen, "A Study On The Changes In Microstructure And Mechanical Properties Of Multi-Pass Welding Between 316 Stainless Steel And Low-Carbon Steel," *J. Adv. Manuf. Technol.*, vol. 12, no. 2, pp. 25–40, 2018.

[8] Q. Gao *et al.*, "Effect mechanism of cryogenic treatment on ferroalloy and nonferrous alloy and their weldments: a review," *Mater. Today Commun.*, p. 104830, 2022.

[9] H. E. Boyer, "Heat treating of nonferrous alloys." Springer, 2013.

[10] X. . Pham, A. . Hoang, and D. . Nguyen, "A study on the effect of the change of tempering temperature on the microstructure transformation of Cu-Ni-Sn alloy," *Int. J. Mech. Mechatronics Eng.*, vol. 18, no. 4, pp. 27–34, 2018.

[11] D. N. Nguyen, A. T. Hoang, M. T. Sai, M. Q. Chau, and V. V. Pham, "Effect of Sn component on properties and microstructure Cu-Ni-Sn alloys," *J. Teknol.*, vol. 80, no. 6, pp. 43–51, 2018.

[12] D. M. Fellicia, M. I. P. Hidayat, R. Rochiem, L. B. A. Putra, A. T. Wibisono, and M. Ramadhani, "Modeling and Experimental Study of Al-Cu Alloy Sand Casting for Circuit Breaker," *Int. J. Adv. Sci. Eng. Inf. Technol.*, vol. 9, no. 3, pp. 880–887, 2019.

[13] X. D. Pham, A. T. Hoang, D. N. Nguyen, and V. V Le, "Effect of Factors on the Hydrogen Composition in the Carburizing Process," *Int. J. Appl. Eng. Res.*, vol. 12, no. 19, pp. 8238–8244, 2017.

[14] A. T. Hoang, T. T. Van Tran, V. B. Nguyen, and D. N. Nguyen, "Effect of Heat Treatment Process on The Microstructure and Mechanical

Properties of The Spray Coating Ni-Cr on CT38 Steel," *Int. J. Adv. Sci. Eng. Inf. Technol.*, vol. 9, no. 2, pp. 560–568, Mar. 2019, doi:10.18517/ijaseit.9.2.7891.

[15] T. X. Tran *et al.*, "Effect of poly-alkylene-glycol quenchant on the distortion, hardness, and microstructure of 65Mn steel," *C. Mater. Contin.*, vol. 67, no. 3, pp. 3249–3264, 2021.

[16] A. T. Hoang *et al.*, "Thermodynamic Simulation on the Change in Phase for Carburizing Process," *C. Mater. Contin.*, vol. 68, no. 1, pp. 1129–1145, 2021.

[17] H. Thi, N. Quyen, V. A. Tuan, T. P. Dong, V. V. Quyen, and N. D. Nam, "Effect of Rare Earth on M7C3 Eutectic Carbide in 13 % Chromium Alloy Cast Iron," *Int. J. Adv. Sci. Eng. Inf. Technol.*, vol. 9, no. 2, pp. 724–728, 2019.

[18] A. Fuad *et al.*, "Effects of Laminate Arrangement on the Failure Behaviour of Hybrid Composite Plates under Transverse Sinusoidal Load," *Int. J. Adv. Sci. Eng. Inf. Technol.*, vol. 9, no. 3, pp. 799–803, 2019.

[19] F. Khathyri, B. Elkihel, and F. Delaunois, "Non-Destructive Testing by Ultrasonic and Thermal Techniques of an Impacted Composite Material," *Int. J. Adv. Sci. Eng. Inf. Technol.*, vol. 8, no. 6, pp. 2360–2366, 2018.

[20] S. Hou *et al.*, "Facile fabrication of flexible superhydrophobic surfaces with high durability and good mechanical strength through embedding silica nanoparticle into polymer substrate by spraying method," *Colloids Surfaces A Physicochem. Eng. Asp.*, vol. 664, p. 131181, 2023.

[21] M. J. Chinchillas-Chinchillas *et al.*, "Evaluation of the mechanical properties, durability and drying shrinkage of the mortar reinforced with polyacrylonitrile microfibers," *Constr. Build. Mater.*, vol. 210, pp. 32–39, 2019.

[22] R. M. Bajracharya, A. C. Manalo, W. Karunasena, and K. Lau, "An overview of mechanical properties and durability of glass-fibre reinforced recycled mixed plastic waste composites," *Mater. Des.*, vol. 62, pp. 98–112, 2014.

[23] M. K. Pham, D. N. Nguyen, and A. T. Hoang, "Influence of Vanadium Content on the Microstructure and Mechanical Properties of High-Manganese Steel," *Int. J. Mech. Mechatronics Eng.*, vol. 18, no. 2, pp. 141–147, 2018.

[24] M. Abid, M. Kchaou, A. T. Hoang, and M. Haboussi, "Wear Mechanisms Analysis and Friction Behavior of Anodic Aluminum Oxide Film 5083 under Cyclic Loading," *J. Mater. Eng. Perform.*, vol. 33, no. 3, pp. 1527–1537, Aug. 2024, doi: 10.1007/s11665-023-08616-8.

[25] International Iron and Steel Committee on Automotive Applications, "Advanced High Strength Steels (AHSS) Application Guidelines," 2005.

[26] M. Y. Demeri, *Advanced high-strength steels: science, technology, and applications*. ASM international, 2013.

[27] N. V. L. Le, D. N. Nguyen, A. T. Vu, D. T. Nguyen, and T. T. T. Tran, "Review on bainite phase transformation and mechanism in CMnSi steel," in *AIP Conference Proceedings*, AIP Publishing, 2023.

[28] V. F. Zackay, E. R. Parker, D. Fahr, and R. Busch, "The enhancement of ductility in high-strength steels," *ASM Trans Quart*, vol. 60, no. 2, pp. 252–259, 1967.

[29] P. I. Christodoulou, "Effect of retained austenite transformation on the fatigue behaviour of aluminum containing TRIP steels." Doctoral dissertation, University of Thessaly, 2018.

[30] J. Zhao and Z. Jiang, "Thermomechanical processing of advanced high strength steels," *Prog. Mater. Sci.*, vol. 94, pp. 174–242, 2018.

[31] S. Hashimoto, S. Ikeda, K. Sugimoto, and S. Miyake, "Effects of Nb and Mo addition to 0.2% C-1.5% Si-1.5% Mn steel on mechanical properties of hot rolled TRIP-aided steel sheets," *ISIJ Int.*, vol. 44, no. 9, pp. 1590–1598, 2004.

[32] L. Skálová, R. Divišová, and D. Jandová, "Thermo-mechanical processing of low-alloy TRIP-steel," *J. Mater. Process. Technol.*, vol. 175, no. 1–3, pp. 387–392, 2006.

[33] E. Erişir, O. G. Bilir, Y. E. Sözer, Ö. Ararat, and K. Davut, "Partial austenitisation and TBF steel composed of ferrite, bainitic ferrite, and austenite," *Mater. Sci. Technol.*, vol. 39, no. 1, pp. 105–116, 2023.

[34] S. Traint, A. Pichler, M. Blaimschein, B. Röthler, C. Krempaszky, and E. Werner, "Alloy design, processing and properties of TRIP steels: A critical comparison," in *International Conference on Advanced High Strength Sheet Steels for Automotive Applications - Proceedings*, 2004.

[35] B. Sunil and S. Rajanna, "Evaluation of mechanical properties of ferrite-martensite DP steels produced through intermediate quenching technique," *SN Appl. Sci.*, vol. 2, no. 8, 2020, doi: 10.1007/s42452-020-03246-4.

[36] S. Qin, Y. Lu, S. B. Sinnott, and A. M. Beese, "Influence of phase and interface properties on the stress state dependent fracture initiation behavior in DP steels through computational modeling," *Mater. Sci. Eng. A*, vol. 776, 2020, doi: 10.1016/j.msea.2020.138981.

[37] D. Van Hien, "Influence of thermal-mechanical on microstructure and mechanical of TRIP CMnSi Steel from foam-iron," Institute of Military Science and Technology, 2018.

[38] M. Soleimani, H. Mirzadeh, and C. Dehghanian, "Effects of tempering on the mechanical and corrosion properties of dual phase steel," *Mater. Today Commun.*, vol. 22, 2020, doi: 10.1016/j.mtcomm.2019.100745.

[39] B. Fu, W. Y. Yang, M. Y. Lu, Q. Feng, L. F. Li, and Z. Q. Sun, "Microstructure and mechanical properties of C-Mn-Al-Si hot-rolled TRIP steels with and without Nb based on dynamic transformation," *Mater. Sci. Eng. A*, vol. 536, pp. 265–268, 2012, doi:10.1016/j.msea.2012.01.012.

[40] I. Samajdar, E. Girault, B. Verlinden, E. Aernoudt, and J. Van Humbeeck, "Transformations during intercritical annealing of a TRIP-assisted steel," *ISIJ Int.*, vol. 38, no. 9, 1998, doi:10.2355/isijinternational.38.998.

[41] P. J. Jacques, "Transformation-induced plasticity for high strength formable steels," *Curr. Opin. Solid State Mater. Sci.*, vol. 8, no. 3–4, 2004, doi: 10.1016/j.cossms.2004.09.006.

[42] H. D. Van, C. N. Van, T. T. Ngoc, and T. S. Manh, "ScienceDirect Influence of heat treatment on microstructure and mechanical properties of a CMnSi TRIP steel using design of experiment," vol. 00, 2017.

[43] A. Kupke, "Effect of the microstructure on the unloading characteristics of DP steel," Deakin University, 2016.

[44] H. K. D. H. Bhadeshia, *Bainite in steels*, 2nd Editio. Cambridge University: Institute of Materials, 2001.

[45] Yang Z-G, Fang H-S. "An overview on bainite formation in steels*,*" *Curr Opin Solid State Mater Sci.*, 9, pp.277–86, 2005.

[46] H. Takechi, "Transformation hardening of steel sheet for automotive applications," *JOM*, vol. 60, no. 12, 2008, doi: 10.1007/s11837-008-0160-6.

[47] R. L. Bodnar, T. Ohhashi, and R. I. Jaffee, "Errata: Effects of Mn, Si, and purity on the design of 3.5NiCrMoV, 1CrMoV, and 2.25Cr-1Mo bainitic alloy steels," *Metallurgical Transactions A*, vol. 20, no. 10. 1989. doi: 10.1007/BF02650311.

[48] T. T. T. Van Le Van Cuong, Nguyen Anh Xuan, Le Thi Nhung, *Material Engineering*. Vimaru publisher, 2017.

[49] A. M. Ravi, A. Navarro-López, J. Sietsma, and M. J. Santofimia, "Influence of martensite/austenite interfaces on bainite formation in low-alloy steels below Ms," *Acta Mater.*, vol. 188, 2020, doi:10.1016/j.actamat.2020.02.003.

[50] S. M. Hasan, S. Kumar, D. Chakrabarti, and S. B. Singh, "Effect of prior austenite grain size on the formation of carbide-free bainite in low-alloy steel," *Philos. Mag.*, vol. 100, no. 18, 2020, doi:10.1080/14786435.2020.1764653.

[51] S. Keeler and M. Kimchi, "Advanced High-Strength Steels Application Guidelines Version 5.0," *World AutoSteel.org*, no. May, p. 511, 2014, doi: 10.1016/S1644-9665(12)60197-6.

[52] Y. Tomota *et al.*, "Tensile behavior of TRIP-aided multi-phase steels studied by in situ neutron diffraction," *Acta Mater.*, vol. 52, no. 20, 2004, doi: 10.1016/j.actamat.2004.08.016.

[53] C. G. Lee, S. J. Kim, C. S. Oh, and S. Lee, "Effects of heat treatment and Si addition on the mechanical properties of 0.1 wt% C TRIP-aided cold-rolled steels," *ISIJ Int.*, vol. 42, no. 10, pp. 1162–1168, 2002, doi: 10.2355/isijinternational.42.1162.

[54] S. Allain and A. Perlade, "Applications Why developing Advanced High Strength Steels".

[55] L. J. Zhu, D. Wu, and X. M. Zhao, "Effect of silicon addition on recrystallization and phase transformation behavior of high-strength hot-rolled trip steel," *Acta Metall. Sin. (English Lett.)*, vol. 21, no. 3, pp. 163–168, 2008, doi: 10.1016/S1006-7191(08)60034-4.

[56] A. Berezovski and G. Maugin, "Thermodynamics of Discrete Systems and Martensitic Phase Transition Simulation," 2001.

[57] C. Garcia-Mateo, T. Sourmail, F. G. Caballero, C. Capdevila, and C. De García Andrés, "New approach for the bainite start temperature calculation in steels," *Mater. Sci. Technol.*, vol. 21, no. 8, pp. 934–940, Aug. 2005, doi: 10.1179/174328405X51622.

[58] Y. Esparza, A. Ullah, Y. Boluk, and J. Wu, "Preparation and characterization of thermally crosslinked poly(vinyl alcohol)/feather keratin nanofiber scaffolds," *Mater. Des.*, vol. 133, 2017, doi: 10.1016/j.matdes.2017.07.052.

[59] H. C. Chen, H. Era, and M. Shimizu, "Effect of phosphorus on the formation of retained austenite and mechanical properties in Si-

containing low-carbon steel sheet," *Metall. Trans. A*, vol. 20, no. 3, pp. 437–445, Mar. 1989, doi: 10.1007/BF02653923.

[60] L. C. D. Fielding, "The bainite controversy," *Materials Science and Technology (United Kingdom)*, vol. 29, no. 4. 2013. doi:10.1179/1743284712Y.0000000157.

[61] L. C. Duong, *Material Science*. Science and Engineerinh Publisher - Hanoi, 2000.

[62] L. Leach, *Modeling Bainite Formation in Steels*. KTH Royal Institute of Technology, 2018.

[63] H. Matsuda and H. K. D. H. Bhadeshia, "Kinetics of the bainite transformation," *Proc. R. Soc. A Math. Phys. Eng. Sci.*, vol. 460, no. 2046, pp. 1707–1722, Jun. 2004, doi: 10.1098/rspa.2003.1225.

[64] J. Ågren, "Thermodynamics of phase transformations in steels," in *Phase Transformations in Steels*, vol. 1, Elsevier Ltd, 2012, pp. 56–93. doi: 10.1533/9780857096104.1.56.

[65] D. Quidort and Y. J. M. Brechet, "Isothermal growth kinetics of bainite in 0.5% C steels," *Acta Mater.*, vol. 49, no. 20, 2001, doi:10.1016/S1359-6454(01)00316-0.

[66] D. Ponge, Z. Peng, A. J. Breen, and K. Analysis, "Phase nucleation through con fi ned spinodal fl uctuations at crystal defects evidenced in Fe-Mn alloys," no. March, 2018, doi:10.1038/s41467-018-03591-4.

[67] R. Trivedi and G. M. Pound, "Growth kinetics of plate-like precipitates," *J. Appl. Phys.*, vol. 40, no. 11, 1969, doi:10.1063/1.1657190.

[68] J. I. Goldstein, *Phase Transformations in Ferrous Alloys*. 1984.

[69] G. I. Rees and H. K. D. H. Bhadeshia, "Bainite transformation kinetics Part 1 Modified model," *Mater. Sci. Technol. (United Kingdom)*, vol. 8, no. 11, 1992, doi: 10.1179/mst.1992.8.11.985.

[70] Fisher M, Radin C. *Definition of Thermodynamic Phases and Phase Transitions*. 2006.

[71] M. Enomoto, G. Spanos, and R. A. Masumura, "The Growth Kinetics and Shape Evolution of Precipitates Growing by the Ledge Mechanism," *MRS Proc.*, vol. 237, 1991, doi: 10.1557/proc-237-119.

[72] B. Verlinden, J. Driver, I. Samajdar, and R. D. Doherty, *Thermo-mechanical processing of metallic materials*. Elsevier, 2007.

[73] M. Soleimani, A. Kalhor, and H. Mirzadeh, "Transformation-induced plasticity (TRIP) in advanced steels: A review," *Mater. Sci. Eng. A*, vol. 795, p. 140023, 2020.

[74] S. X. Zhao, W. Wang, and D. L. Mao, "On Bainite Transformation Kinetics and Mechanism," *Mater. Sci. Forum*, vol. 539–543, 2007, doi: 10.4028/www.scientific.net/msf.539-543.3018.

[75] E. P. Simonen, H. I. Aaronson, and R. Trivedi, "Lengthening kinetics of ferrite and bainite sideplates," *Metall. Trans.*, vol. 4, no. 5, 1973, doi: 10.1007/BF02644517.

[76] Pereloma, E., & Edmonds, D. Phase transformations in steels. Fundamentals and diffusion-controlled transformations, (1st ed., vol. 1), Woodhead Publishing, 2012.

[77] Z. cheng Zhang, F. xian Zhu, and Y. mei Li, "Effect of Thermomechanical Control Processing on Microstructure and Mechanical Properties of Fe-0. 2C-1. 44Si-1. 32Mn Hot Rolled TRIP Steel," *J. Iron Steel Res. Int.*, vol. 17, no. 7, pp. 44–50, 2010, doi:10.1016/S1006-706X(10)60155-0.

[78] A. S. M. I. Handbook, "ASM handbook (Heat treating of Irons and Steels)," *ASM Int.*, 2005.

[79] H. K. D. H. Bhadeshia, "Nucleation of Burst Martensite," *Journal of Materials Science*, vol. 17. pp. 383–386, 1982.

[80] S. Chatterjee and H. K. D. H. Bhadeshia, "TRIP-assisted steels: Cracking of high-carbon martensite," *Mater. Sci. Technol.*, vol. 22, no. 6, pp. 645–649, 2006, doi: 10.1179/174328406X86182.

[81] H. L. Yi, S. K. Ghosh, H. Bhadeshia, and K. Y. Lee, "δ-TRIP Steel," *Pohang Pohang Univ. Sci. Technol.*, 2010.

[82] S. Chatterjee and H. K. D. H. Bhadeshia, "Transformation induced plasticity assisted steels: Stress or strain affected martensitic transformation?," *Mater. Sci. Technol.*, vol. 23, no. 9, pp. 1101–1104, Sep. 2007, doi: 10.1179/174328407X226536.

[83] S. Chatterjee, M. Muruganannth, and H. K. D. H. Bhadeshia, "δ TRIP steel," *Mater. Sci. Technol.*, vol. 23, no. 7, pp. 819–827, 2007, doi: 10.1179/174328407X179746.

[84] A. Saha Podder and H. K. D. H. Bhadeshia, "Thermal stability of austenite retained in bainitic steels," *Mater. Sci. Eng. A*, vol. 527, no. 7–8, pp. 2121–2128, 2010, doi: 10.1016/j.msea.2009.11.063.

[85] H. L. Yi, K. Y. Lee, and H. K. D. H. Bhadeshia, "Extraordinary ductility in Al-bearing δ-TRIP steel," *Proc. R. Soc. A Math. Phys. Eng. Sci.*, vol. 467, no. 2125, pp. 234–243, 2011, doi:10.1098/rspa.2010.0127.

[86] X. J. Jin *et al.*, "High Strength Steels Treated by Quenching and Partitioning Process Location and Figures," 2010.

[87] H. K. D. H. Bhadeshia and D. V. Edmonds, "Tempered Martensite Embrittlement: Role of Retained Austenite and Cementite.," *Met Sci*, vol. 13, no. 6. pp. 325–334, 1979.

[88] A. S. Podder, I. Lonardelli, A. Molinari, and H. K. D. H. Bhadeshia, "Thermal stability of retained austenite in bainitic steel: An in situ study," *Proc. R. Soc. A Math. Phys. Eng. Sci.*, vol. 467, no. 2135, pp. 3141–3156, 2011, doi: 10.1098/rspa.2011.0212.

[89] S. Jamshaid, *Materials Engineering and Science an Introduction To Materials Engineering and Science for Chemical and Materials Engineers*, no. November 2013. 2016.

[90] W. D. Callister, *Materials Science and Engineering*, vol. 7. 2007.

[91] Ley Organica de Salud, "No Titleكتاب," *Vasc. Embolotherapy*, pp. 107–118, 2006.

[92] M. A. Yescas and H. K. D. H. Bhadeshia, "Model for the maximum fraction of retained austenite in austempered ductile cast iron," *Mater. Sci. Eng. A*, vol. 333, no. 1–2, pp. 60–66, 2002, doi: 10.1016/S0921-5093(01)01840-8.

[93] Dowling NE. Mean stress effects in stress-life and strain-life fatigue. *SAE Technical Paper*; 2004.

[94] G. Papadimitriou and J. M. R. Genin, "Kinetic and Thermodynamic Aspects of The Bainite Reaction in A Silicon Steel.," in *Materials Research Society Symposia Proceedings*, 1984. doi: 10.1557/proc-21-747.

[95] S. AA, "Thermodynamic Calculation of a Heat of First-Order Phase Transitions," *J. Thermodyn. Catal.*, vol. 7, no. 2, 2016, doi: 10.4172/2157-7544.1000163.

[96] X. L. Wan, R. Wei, L. Cheng, M. Enomoto, and Y. Adachi, "Lengthening kinetics of ferrite plates in high-strength low-carbon low alloy steel," *J. Mater. Sci.*, vol. 48, no. 12, 2013, doi: 10.1007/s10853-013-7250-8.

[97] Fultz B. *Phase transitions in materials*. Cambridge University Press; 2020.

[98] I. K. Razumov, Y. N. Gornostyrev, and M. I. Katsnelson, "Towards the ab initio-based theory of phase transformations in iron and steel," *Phys. Met. Metallogr.*, vol. 118, pp. 362–388, 2017.

[99] G. I. Rees and H. K. D. H. Bhadeshia, "Bainite transformation kinetics Part 1 Modified model," *Mater. Sci. Technol.*, vol. 8, no. 11, 2012, doi:10.1179/026708392790409842.

[100] Z. Chen, J. Gu, and L. Han, "Bainite Transformation Characteristics of High-Si Hypereutectoid Bearing Steel," *Metallogr. Microstruct. Anal.*, vol. 7, no. 1, 2018, doi: 10.1007/s13632-017-0410-5.

[101] H. L. Yi, K. Y. Lee, and H. K. D. H. Bhadeshia, "Stabilisation of ferrite in hot rolled d-TRIP steel," *Mater. Sci. Technol.*, vol. 27, no. 2, pp. 525–529, 2011, doi: 10.1179/026708309X12506934374001.

[102] G. S. Jung, K. Y. Lee, J. B. Lee, H. K. D. H. Bhadeshia, and D. W. Suh, "Spot weldability of TRIP assisted steels with high carbon and aluminium contents," *Sci. Technol. Weld. Join.*, vol. 17, no. 2, pp. 92–98, 2012, doi: 10.1179/1362171811Y.0000000081.

[103] M. Marimuthu, "Design of welding alloys creep and toughness," no. November, pp. 1–187, 2002.

[104] H. L. Yi, K. Y. Lee, and H. K. D. H. Bhadeshia, "Mechanical stabilisation of retained austenite in δ-TRIP steel," *Mater. Sci. Eng. A*, vol. 528, no. 18, pp. 5900–5903, 2011, doi:10.1016/j.msea.2011.03.111.

[105] S. H. Hendi, S. Panahiyan, B. E. Panah, and M. Jamil, "Alternative approach to thermodynamic phase transitions," *Chinese Phys. C*, vol. 43, no. 11, 2019, doi: 10.1088/1674-1137/43/11/113106.

[106] M. Cottura, B. Appolaire, A. Finel, and Y. Le Bouar, "Plastic relaxation during diffusion-controlled growth of Widmanstätten plates," *Scr. Mater.*, vol. 108, 2015, doi:10.1016/j.scriptamat.2015.06.032.

[107] R. E. Smallman and R. J. BiShop, "Chapter 4 - Defects in solids," *Mod. Phys. Metall. Mater. Eng. (Sixth Ed.)*, pp. 84–124, 1999.

[108] B. C. De Cooman, "Structure–properties relationship in TRIP steels containing carbide-free bainite," *Curr. Opin. Solid State Mater. Sci.*, vol. 8, no. 3–4, pp. 285–303, 2004.

[109] M. Rettenmayr, "Alloy development using modern tools," *Int. J. Mater. Res.*, vol. 100, no. 2, pp. 153–159, 2009.

[110] R. W. Cahn and P. Haasen, *Physical metallurgy*, vol. 1. Elsevier, 1996.

[111] R.E. Smallman and R.J. Bishop, *Modern Physical Metallurgy and Materials Engineering*. 1999.

[112] R. E. Smallman and R. J. Bishop, "The structure and bonding of atoms," *Mod. Phys. Metall. Mater. Eng.*, pp. 1–10, 1999, doi:10.1016/b978-075064564-5/50001-x.

[113] H. K. D. H. Bhadeshia and D. V. Edmonds, "The Distribution of Retained Austenite in MArtensite and the Influence of Inter-lath Crystallography," *Proc. Int. Conf. on Martensitic Transformations*. pp. 28–33, 1979.

[114] R. E. Smallman and R. J. Bishop, "The characterization of materials," *Mod. Phys. Metall. Mater. Eng.*, pp. 125–167, 1999, doi:10.1016/b978-075064564-5/50005-7.

[115] R. E. Smallman and R. J. Bishop, Structural phases: Their formation and transitions. Oxford, UK: Butterworth-Heinemann, 1999.

[116] ASM International Handbook Committee, "ASM Handbook: Materials Characterization, Volume 10," *Book*, 1998.

[117] A. Rollett, F. Humphreys, G. S. Rohrer, and M. Hatherly, "Recrystallization and Related Annealing Phenomena - Chapter 3 - Deformation Textures," *Recryst. Relat. Annealing Phenom.*, 2017, doi:10.1016/B978-0-08-098235-9.00003-3.

[118] B. Fu, W. Yang, L. Li, and Z. Sun, "Effect of carbon content on microstructure and mechanical properties of cold-rolled C-Mn-Al-Si trip steel," *Jinshu Xuebao/Acta Metall. Sin.*, vol. 49, no. 4, 2013, doi:10.3724/SP.J.1037.2012.00656.

[119] H. Nasr El-Din, E. A. Showaib, N. Zaafarani, and H. Refaiy, "Structure-properties relationship in TRIP type bainitic ferrite steel austempered at different temperatures," *Int. J. Mech. Mater. Eng.*, vol. 12, no. 1, p. 3, Dec. 2017, doi: 10.1186/s40712-017-0071-9.

[120] R. W. K. Honeycombe and R. F. Mehl, "Transformation from austenite in alloy steels," *Metall. Trans. A*, pp. 915–936, 1976.

[121] T. Minote, S. Torizuka, A. Ogawa, and M. Niikura, "Modeling of Transformation Behavior and Compositional Partitioning in TRIP Steel.," *ISIJ Int.*, vol. 36, no. 2, pp. 201–207, 1996, doi:10.2355/isijinternational.36.201.

[122] F. C. Campbell, *Elements of metallurgy and engineering alloys*. ASM international, 2008.

[123] N. N. Linh, P. T. Bình, T. V. Đoàn, and Đ. B. Trụ, "Các kết quả nghiên cứu ứng dụng về sản xuất sắt xốp Mirex và thép hợp kim," in *Hội nghị KH&CN toàn quốc về cơ khí lần thứ III*, 2013.

[124] S. C. Baik, S. Kim, Y. S. Jin, and O. Kwon, "Effects of Alloying Elements on Mechanical Properties and Phase Transformation of Cold Rolled TRIP Steel Sheets.," *ISIJ Int.*, vol. 41, no. 3, pp. 290–297, 2001, doi: 10.2355/isijinternational.41.290.

[125] W. Bleck, A. Frehn, and J. Ohlert, "Niobium in dual phase and trip steels," *Niobium–Science Technol. Proceedings. Niobium*, pp. 727–752, 2001.

[126] N. Low and N. Grain, "7.4.10 Kinetics of strain-ageing," no. 2, 1960.

[127] S. M. C. van Bohemen, "Bainite and martensite start temperature calculated with exponential carbon dependence," *Mater. Sci. Technol.*, 2013.

[128] Y. Wang *et al.*, "Enhanced stretch flangeability and crack propagation behavior of an 1100áMPa grade TRIP-aided bainitic ferrite steel," *J. Mater. Res. Technol.*, vol. 26, pp. 5503–5517, 2023.

[129] T. Furuhara, K. Tsuzumi, G. Miyamoto, T. Amino, and G. Shigesato, "Characterization of Transformation Stasis in Low-Carbon Steels Microalloyed with B and Mo," *Metall. Mater. Trans. A Phys. Metall. Mater. Sci.*, vol. 45, no. 13, 2014, doi: 10.1007/s11661-014-2584-7.

[130] N. V. Luzginova, L. Zhao, and J. Sietsma, "Bainite formation kinetics in high carbon alloyed steel," *Mater. Sci. Eng. A*, vol. 481–482, no. 1-2 C, 2008, doi: 10.1016/j.msea.2006.11.173.

[131] F. Hardesty, "Metals handbook, ninth edition. Volume 3, Properties and selection: Stainless steels, tool materials and special-purpose metals," *J. Mech. Work. Technol.*, vol. 6, no. 4, 1982, doi:10.1016/0378-3804(82)90039-0.

[132] Junya Kobayashi, "A basic study on the microstructure and mechanical properties of ultrahigh-strength TRIP-aided martensitic steel Junya Kobayashi," 2014.

[133] K. F. Rodrigues, G. M. M. Mourão, and G. L. Faria, "Kinetics of Isothermal Phase Transformations in Premium and Standard Rail Steels," *Steel Res. Int.*, vol. 92, no. 2, Feb. 2021, doi: 10.1002/srin.202000306.

[134] A. M. Ravi, J. Sietsma, and M. J. Santofimia, "Exploring bainite formation kinetics distinguishing grain-boundary and autocatalytic nucleation in high and low-Si steels," *Acta Mater.*, vol. 105, 2016, doi: 10.1016/j.actamat.2015.11.044.

[135] W. Yan, N. Xiao, Y. Chen, and D. Li, "Phase-field modeling of Widmanstätten ferrite formation during isothermal transformation in low carbon steels," *Comput. Mater. Sci.*, vol. 81, 2014, doi:10.1016/j.commatsci.2013.09.001.

[136] W. Steven and A. G. Haynes, "The Temperature of Formation of Martensite and Bainite in Low-alloy Steels - Some Effects of Chemical Composition," *J. Iron Steel Inst.*, vol. 183, 1956.

[137] T. Hojo, J. Kobayashi, T. Kajiyama, and K. Sugimoto, "Effects of Alloying Elements on Impact Properties of Ultra High-Strength TRIP-Aided Bainitic Ferrite Steels," pp. 9–16.

[138] N. Fonstein, *Advanced High Strength Sheet Steels*. 2015. doi:10.1007/978-3-319-19165-2.

[139] D. O. C. Tor, *Structure and Properties of Advanced Fine Grained Steels Produced Using Novel Thermal Treatments*.

[140] P. J. Jacques, Q. Furnemont, S. Godet, T. Pardoen, K. T. Conlon, and F. Delannay, "Micromechanical characterisation of TRIP-assisted multiphase steels by in situ neutron diffraction," *Philos. Mag.*, vol. 86, no. 16, 2006, doi: 10.1080/14786430500529359.

[141] R. Kuziak, R. Kawalla, and S. Waengler, "Advanced high strength steels for automotive industry," *Arch. Civ. Mech. Eng.*, vol. 8, no. 2, pp. 103–117, 2008.

[142] M. Azuma, M. Takahashi, and N. Fujita, "Model for the Prediction of Microstructures and Mechanical Properties of Cold-rolled High Strength Steels," *Nippon Steel Tech. Rep.*, no. 102, pp. 44–50, 2013.

[143] A. A. Shirzadi, H. K. D. H. Bhadeshia, L. Karlsson, and P. J. Withers, "Stainless steel weld metal designed to mitigate residual stresses," *Sci. Technol. Weld. Join.*, vol. 14, no. 6, pp. 559–565, 2009, doi: 10.1179/136217109X437178.

[144] H. Halfa, "Recent Trends in Producing Ultrafine Grained Steels," *J. Miner. Mater. Charact. Eng.*, vol. 02, no. 05, 2014, doi:10.4236/jmmce.2014.25047.

[145] Z. Zhao, C. Liu, Y. Liu, and D. O. Northwood, "A new empirical formula for the bainite upper temperature limit of steel," *J. Mater. Sci.*, vol. 36, no. 20, 2001, doi: 10.1023/A:1011874708194.

[146] S. Kang, S. Yoon, and S. J. Lee, "Prediction of bainite start temperature in alloy steels with different grain sizes," *ISIJ Int.*, vol. 54, no. 4, 2014, doi: 10.2355/isijinternational.54.997.

[147] J. Hren, *Introduction to analytical electron microscopy*. Springer Science & Business Media, 2013.

[148] D. François, A. Pineau, and A. Zaoui, *Mechanical behaviour of materials*, vol. 1. Springer, 1998.

[149] J. J. Zhao, Y. L. He, N. Q. Zhu, M. Zhang, and L. Li, "Thermodynamic calculation and experimental study on complex phase steel," in *Advanced Materials Research*, 2013, pp. 349–354. doi:10.4028/www.scientific.net/AMR.716.349.

[150] M. De Meyer, D. Vanderschueren, and B. De Cooman, "The Influence of Al on the Properties of Cold Rolled C-Mn-Si TRIP Steels.," in *ISS, 41st Mechanical Working and Steel Processing Conference, 24-27/10/99, Baltimore, Vol. XXXXVII.*, 1999, pp. 265–276.

[151] D. Krizan and B. C. D. E. Cooman, "Mechanical Properties of TRIP Steel Microalloyed with Ti Mechanical Properties of TRIP Steel Microalloyed with Ti," no. July, 2014, doi:10.1007/s11661-014-2292-3.

[152] T. Fukagawa, H. Okada, and Y. Maehara, "Mechanism of Red Scale Defect Formation in Si-added Hot-rolled Steel Sheets.," *ISIJ Int.*, vol. 34, no. 11, pp. 906–911, 1994, doi:10.2355/isijinternational.34.906.

[153] J. B. R. Lawrence, "The effect of phase morphology and volume fraction of retained austenite on the formability of transformation induced plasticity steels," Queen's University, 2010.

[154] J. Drumond, O. Girina, J. F. da Silva Filho, N. Fonstein, and C. A. S. de Oliveira, "Effect of Silicon Content on the Microstructure and Mechanical Properties of Dual-Phase Steels," *Metallogr. Microstruct. Anal.*, vol. 1, no. 5, pp. 217–223, Oct. 2012, doi: 10.1007/s13632-012-0034-8.

[155] N. D. Nam, T. P. Dong, T. T. Nam, N. H. Hai, and P. M. Khanh, "Influence of the Deformation on the Microstructure and Mechanical Properties of TBF Steel," *J. Korean Soc. Precis. Eng.*, vol. 37, no. 8, pp. 595–600, Aug. 2020, doi: 10.7736/JKSPE.019.054.

[156] I. D. Choi *et al.*, "Deformation Behavior of Low Carbon TRIP Sheet Steels at High Strain Rates.," *ISIJ Int.*, vol. 42, no. 12, pp. 1483–1489, 2002, doi: 10.2355/isijinternational.42.1483.

[157] O. Matsumura, Y. Sakuma, and H. Takechi, "Enhancement of elongation by retained austenite in intercritical annealed 0.4C-1.5Si-0.8Mn steel.," *Trans. Iron Steel Inst. Japan*, vol. 27, no. 7, pp. 570–579, 1987, doi: 10.2355/isijinternational1966.27.570.

[158] J. Zrnik, O. Stejskal, Z. Novy, and P. Hornak, "Relationship of microstructure and mechanical properties of TRIP-aided steel processed by press forging," *J. Mater. Process. Technol.*, vol. 192–193, pp. 367–372, Oct. 2007, doi: 10.1016/j.jmatprotec.2007.04.012.

[159] A. Bachmaier, K. Hausmann, D. Krizan, and A. Pichler, "Development of TBF steels with 980 MPa tensile strength for automotive applications: microstructure and mechanical properties," in *Proceedings of the International Symposium on New Developments in Advanced High Strength Sheet Steels, Vail, CO, USA*, 2013, pp. 23–27.

[160] S.-C. Chen, Y.-T. Wang, Y.-C. Lin, C.-Y. Huang, J.-R. Yang, and H.-W. Yen, "Microstructure and mechanical behaviors of GPa-grade TRIP steels enabled by hot-rolling processes," *Mater. Sci. Eng. A*, vol. 761, p. 138005, 2019.

324

[161] L. Qian *et al.*, "Enhancing both strength and ductility of low-alloy transformation-induced plasticity steel via hierarchical lamellar structure," *Scr. Mater.*, vol. 183, pp. 96–101, 2020.

[162] T. Murata, S. Hamamoto, Y. Utsumi, T. Yamano, Y. Futamura, and T. Kimura, "Characteristics of 1180 MPa grade cold-rolled steel sheets with excellent formability," *Kobelco Technol. Rev.*, vol. 35, pp. 45–49, 2017.

[163] Y. Li, W. Ding, and B. Wang, "Intercritical annealing pre-treatment used in a hot-dip galvanised TRIP steel," *Mater. Sci. Technol.*, vol. 35, no. 11, pp. 1372–1380, 2019.

[164] T. Hojo *et al.*, "Hydrogen embrittlement resistance of pre-strained ultra-high-strength low alloy TRIP-aided steel," *Int. J. Fract.*, vol. 224, no. 2, pp. 253–260, 2020.

[165] T. Hojo, R. Kikuchi, H. Waki, F. Nishimura, Y. Ukai, and E. Akiyama, "Effect of strain rate on the hydrogen embrittlement property of ultra high-strength low alloy TRIP-aided steel," *Isij Int.*, vol. 58, no. 4, pp. 751–759, 2018.

[166] D. Frómeta *et al.*, "Identification of fracture toughness parameters to understand the fracture resistance of advanced high strength sheet steels," *Eng. Fract. Mech.*, vol. 229, p. 106949, 2020.

[167] T. Hojo, K. Sugimoto, Y. Mukai, and S. Ikeda, "Effects of aluminum on delayed fracture properties of ultra high strength low alloy TRIP-aided steels," *ISIJ Int.*, vol. 48, no. 6, pp. 824–829, 2008.

[168] T. Ruggles *et al.*, "Ductility of advanced high-strength steel in the presence of a sheared edge," *Jom*, vol. 68, pp. 1839–1849, 2016.